

Quantum Non-Linear Bandit Optimization

Zakaria Shams Siam¹, Chaowen Guan², Chong Liu¹

¹University at Albany, State University of New York

²University of Cincinnati

{zsiam, cliu24}@albany.edu, guance@ucmail.uc.edu

Abstract

We study non-linear bandit optimization where the learner maximizes a black-box function with zeroth order function oracle, which has been successfully applied in many critical applications such as drug discovery and materials design. Existing works have showed that with the aid of quantum computing, it is possible to break the classical $\Omega(\sqrt{T})$ regret lower bound and achieve the new $O(\text{poly log } T)$ upper bound. However, they usually assume that the objective function sits within the reproducing kernel Hilbert space and their algorithms suffer from the curse of dimensionality. In this paper, we propose the new Q-NLB-UCB algorithm which enjoys an *input dimension-free* $O(\text{poly log } T)$ upper bound, making it applicable for high-dimensional tasks. At the heart of our algorithm design are quantum Monte Carlo mean estimator, parametric function approximation technique, and a new quantum non-linear regression oracle, which can be of independent interests in more quantum machine learning problems. Our algorithm is also validated for its efficiency compared with other quantum algorithms on both high-dimensional synthetic and real-world tasks.

Code — <https://github.com/ZakSiam/Quantum-Non-Linear-Bandit-Optimization>

Extended version — <https://arxiv.org/abs/2503.03023v2>

Introduction

Non-linear bandit optimization, a.k.a., Gaussian process bandits, kernelized bandits, or Bayesian optimization, is a sequential decision making-based machine learning task that aims at solving a black-box optimization problem. Due to its black-box nature, it has been successfully applied in many important real-world applications where objective functions are difficult to define explicitly, e.g., hyperparameter tuning (Wu et al. 2020), neural architecture search (Kandasamy et al. 2018), drug discovery (Korovina et al. 2020), and materials science (Frazier and Wang 2016).

In drug screening, the objective is to identify a drug candidate from a large pool of compounds that exhibits the highest binding affinity to a specific biological target. Here each candidate is usually described by a feature vector \mathbf{x} and its binding affinity is a function of \mathbf{x} , denoted as $f_0(\mathbf{x})$. Due

to the highly complex chemical and biological reactions, the function f_0 is usually considered “black-box”, which implies that it may be non-linear, non-convex, and even non-differentiable w.r.t. \mathbf{x} . How to optimize f_0 then? The learner is allowed to sequentially query the function f_0 . At each round t , the learner chooses to take a data point \mathbf{x}_t and observes its performance y_t , which is the outcome of a wet lab test. Obviously, a good algorithm can help the learner select promising data points as the experiment progresses and find the best candidate within fewest tests.

In addition to its successful real-world applications, non-linear bandit optimization also enjoys solid theoretical guarantees. In literature, researchers usually define simple regret and cumulative regret to capture the convergence behavior of a certain algorithm, and many regret upper bounds have been established under different assumptions and with different kernels. All these positive theoretical results further contribute to more applications of non-linear bandit optimization. However, unfortunately an $\Omega(\sqrt{T})$ cumulative regret lower bound (Scarlett, Bogunovic, and Cevher 2017) cannot be further improved. What does that mean? It implies that given total T rounds, no algorithm can incur cumulative regret less than $\Omega(\sqrt{T})$ asymptotically.

But can we do better? On the negative side, in classical (non-quantum) setting, the answer is “no”. On the positive side, we have entered the quantum era where the power of quantum computing offers new hope for tackling this challenging optimization problem. (Wan et al. 2023) first studied the multi-armed bandits and linear bandits and proved that new $O(\text{poly log } T)$ regret bound can be achieved with the aid of quantum computing. Later Q-GP-UCB (Dai et al. 2023) and QMCKernelUCB (Hikima et al. 2024) studied the quantum Bayesian optimization, generalizing (Wan et al. 2023) to non-convex and non-linear settings, still achieving the $O(\text{poly log } T)$ regret bound. However, (Dai et al. 2023; Hikima et al. 2024) both heavily rely on the reproducing kernel Hilbert space assumption, which suffers from the curse of dimensionality. The problem is that, in practice, many input data sit in high-dimensional spaces. Again in drug discovery, for example, the dimension of protein sequences usually ranges from thousands (Clarke et al. 2008) to even millions (Rahnenführer et al. 2023). Then either $O(d_x^{\frac{3}{2}}(\log T)^{\frac{3}{2}})$ (linear kernel) or $O(T^{\frac{3d_x}{2v+d_x}})$ (Matérn kernel with v being a

kernel parameter) regret bound (Dai et al. 2023) become vacuous when input dimension d_x goes to millions, which further prevents their high-dimensional real-world applications. Therefore, can we design a new and efficient quantum non-linear bandit optimization algorithm that works well in high-dimensions?

In this paper, we answer this question affirmatively by proposing the Quantum Non-Linear Bandit with Upper Confidence Bound (Q-NLB-UCB) algorithm. The key design of Q-NLB-UCB relies on three techniques. First, Q-NLB-UCB runs in stages where in each stage the quantum oracle associated with the same action will be queried multiple times to achieve the quadratically improved sample complexity, guaranteed by quantum Monte Carlo mean estimator lemma (Montanaro 2015). Second, inspired by the success of parametric function approximation (Liu and Wang 2023), we use a parametric function class to approximate and optimize the black-box objective function. All information queried is handled in the parameter space, so we are able to prove the first input *dimension-free* regret bound for quantum non-linear bandit optimization. Finally, initialization of Q-NLB-UCB relies on a good estimated parameter \hat{w}_0 of the quantum non-linear regression problem. Its convergence to the optimal parameter w^* enjoys a quadratic speed-up rate compared with classical non-linear regression, thanks to the quantum fast-forward technique (Apers and Sarlette 2019).

Contributions. Our contributions are summarized as:

(1) We solve quantum non-linear bandit optimization with quantum computing and parametric function approximation, and propose the new Q-NLB-UCB algorithm. The design of algorithmic framework is generic and the choice of parametric function can be a linear function, quadratic function, or even multi-layer deep neural network, depending on tasks.

(2) Different from existing works, Q-NLB-UCB does not suffer from the curse of dimensionality. We prove the first $O(d_w^2 \log^{\frac{3}{2}}(T) \log(d_w \log T))$ regret bound with d_w being parameter complexity, which is also faster than the classical lower bound $\Omega(\sqrt{T})$ but *independent* to input dimension d_x .

(3) Experiments on high-dimensional synthetic functions and real-world tasks show that Q-NLB-UCB outperforms compared algorithms in regrets and runtime.

Technical Novelties. The design of Q-NLB-UCB is a highly non-trivial task, involving tackling multiple technical challenges. Key technical novelties are highlighted as follows.

(1) The classical $O(1/\sqrt{T_0})$ regression bound (Nowak 2009) with T_0 being number of samples converges too slow to work for Q-NLB-UCB. We introduce the quantum fast-forward technique (Apers and Sarlette 2019) to refine the analysis with Craig-Bernstein inequality (Craig 1933) to work with the quantum non-linear regression oracle, and achieve a *quadratic* improvement in query complexity. This enhancement is highly non-trivial. As far as we know, *no* existing classical or quantum methods can provide a comparable speed-up for the non-linear regression problem. Informally speaking, we prove that there exist such quantum regression solvers attaining this quadratic advantage, shedding light for a specific algorithm design in the future, which can be of independent interests in more quantum machine

learning problems. While classical approaches (Diaconis and Miclo 2013) offer some improvement, they are limited to constant-factor gains, rather than quadratic ones.

(2) In confidence analysis, when constructing the covariance matrix, we take the gradient w.r.t. the fixed initial parameter \hat{w}_0 , rather than \hat{w}_t , which still makes rank-1 updates in each stage but avoids the tedious inductive argument in (Liu and Wang 2023). After the first-order approximation using gradients, multiple parameters sitting in the same convex confidence region are used as bridges to apply convexity properties, ensuring the high-order terms are still well bounded.

Related Work

Classical Optimization. Bayesian optimization (Frazier 2018) is one of the most popular methods to solve global optimization. Based on the Gaussian process (Williams and Rasmussen 2006) or reproducing kernel Hilbert space (Chowdhury and Gopalan 2017) assumption, Bayesian optimization runs in multiple rounds where in each round the learner takes an action suggested by an acquisition function. Common choices of acquisition function include expected improvement (Jones, Schonlau, and Welch 1998), knowledge gradient (Scott, Frazier, and Powell 2011), upper confidence bound (Srinivas et al. 2010), and Thompson sampling (Russo et al. 2018). Without the classical Gaussian process assumption, (Snoek et al. 2015; Springenberg et al. 2016) used neural networks as the backbone surrogate models.

Besides Bayesian optimization, recent bandit works studied global optimization with neural network approximation (Zhou, Li, and Gu 2020; Zhang et al. 2021; Dai et al. 2022) or generic parametric function approximation (Liu and Wang 2023). In addition to bandit optimization, (Wang, Balakrishnan, and Singh 2019) studied the global optimization of an unknown non-convex smooth function. When gradient information is available, (Allen-Zhu 2018; Fang et al. 2018) also proposed algorithms to solve global optimization problem. However, our work is different from all of them since we focus on the quantum bandit optimization.

Quantum Optimization. In recent years, there has been increasing interest in exploring quantum speed-up for optimization problems. This research direction began with quantum algorithms for linear and semi-definite programs (Brandão and Svore 2017; Apeldoorn and Gilyén 2018; Casares and Martin-Delgado 2020; Kerenidis and Prakash 2020), later extending to more general convex optimization (van Apeldoorn et al. 2020; Chakrabarti et al. 2020; He et al. 2022, 2024). Recent advancements include quantum algorithms for slightly convex problems (Li and Zhang 2022; Chen et al. 2025; Zhang et al. 2024), escaping saddle points in non-convex landscapes (Zhang, Leng, and Li 2021; Childs et al. 2022), and identifying global minima in specific non-convex cases (Liu, Su, and Li 2023; Leng et al. 2023). Alongside these algorithmic developments, quantum lower bounds have been established for both convex (Garg et al. 2021b,a) and non-convex optimization (Gong, Zhang, and Li 2025; Zhang and Li 2023).

In a parallel line of research, stochastic quantum methods were proposed (Sidford and Zhang 2023), demonstrating the advantages of quantum stochastic first-order oracles for

smooth objectives in low-dimensional settings. Most recently, there were efforts (Liu et al. 2024) on investigating quantum speed-up for minimizing non-smooth, non-convex objectives, which represent the most general and fundamental function class. At the same time, (Zhang et al. 2024) focused on studying quantum algorithms and lower bounds for finite-sum optimization, addressing both convex and non-convex cases.

Preliminaries

Problem Statement

In this paper, we consider the non-linear bandit optimization problem: $\mathbf{x}^* = \arg \max_{\mathbf{x} \in \mathcal{X}} f_0(\mathbf{x})$, where $f_0 : \mathcal{X} \rightarrow \mathcal{Y}$ is the unknown black-box objective function, which can be non-linear, non-convex, and not necessarily differentiable in \mathbf{x} . $\mathcal{X} \subseteq \mathbf{R}^{d_x}$ is the function domain and $\mathcal{Y} \subseteq \mathbf{R}$ is the function range. To solve this problem, the learner has zeroth-order access to f_0 and the whole process runs in rounds. At each round $t = 1, \dots, T$, after querying action \mathbf{x}_t the oracle will return a noisy function observation y_t . In classical (non-quantum) setting, after taking \mathbf{x}_t , the function returns $y_t = f_0(\mathbf{x}_t) + \eta_t$, where η_t is the zero-mean, independent, σ -sub-Gaussian noise. However, in (bounded value) quantum bandit setting, after taking the same action \mathbf{x}_t multiple times, the function oracle returns y_t that satisfies $|y_t - f_0(\mathbf{x}_t)| \leq \epsilon_t$, where ϵ_t is an error term. Either in classical or quantum setting, throughout T rounds, we can always utilize the cumulative regret to evaluate the optimization process, $R_T = \sum_{t=1}^T f_0(\mathbf{x}^*) - f_0(\mathbf{x}_t)$, where $r_t = f_0(\mathbf{x}^*) - f_0(\mathbf{x}_t)$ is the instantaneous regret at round t . An algorithm \mathcal{A} is said to be a no-regret algorithm if $\lim_{T \rightarrow \infty} R_T(\mathcal{A})/T \rightarrow 0$.

Since we are using a parametric function class to approximate the objective function, we use $\mathcal{W} \subseteq \mathbf{R}^{d_w}$ to denote the parameter class and its corresponding parametric function class is $\mathcal{F} = \{f_{\mathbf{w}} : \mathcal{X} \rightarrow \mathcal{Y} | \mathbf{w} \in \mathcal{W}\}$. Here we abuse the notation since $f_{\mathbf{w}}(\mathbf{x}) = f_{\mathbf{x}}(\mathbf{w})$ and $f_{\mathbf{x}}(\mathbf{w})$ is used when \mathbf{w} is the variable of interest and \mathbf{x} is the parameter, and vice versa. Also, we use $\nabla f_{\mathbf{x}}(\mathbf{w})$ and $\nabla^2 f_{\mathbf{x}}(\mathbf{w})$ denote the gradient vector and Hessian matrix of function w.r.t. \mathbf{w} . For a vector \mathbf{x} , its ℓ_p norm is defined as $\|\mathbf{x}\|_p = (\sum_{i=1}^d |\mathbf{x}_i|^p)^{1/p}$. For a matrix \mathbf{A} , its operator norm is denoted as $\|\mathbf{A}\|_{\text{op}}$. For a vector \mathbf{x} and a matrix \mathbf{A} , let $\|\mathbf{x}\|_{\mathbf{A}}^2 = \mathbf{x}^\top \mathbf{A} \mathbf{x}$. Let $\ell(\cdot, \cdot) : \mathbf{R}^2 \rightarrow \mathbf{R}$ denote a loss function, then the expected risk of a parameter \mathbf{w} is defined as $L(\mathbf{w}) = \mathbf{E}_{(\mathbf{x}, y) \sim \mathcal{D}}[\ell(f_{\mathbf{w}}(\mathbf{x}), y)]$ with respect to distribution \mathcal{D} and the empirical risk of \mathbf{w} is defined as $\hat{L}(\mathbf{w}) = \frac{1}{n} \sum_{i=1}^n \ell(f_{\mathbf{w}}(\mathbf{x}_i), y_i)$ with respect to n data points. For readers' convenience, we use standard big O notation to hide universal constants and use \tilde{O} notation to further hide logarithmic factors.

Quantum Computation

Quantum Basics. A quantum state can be seen as a vector $\mathbf{x} = (x_1, x_2, \dots, x_m)^\top$ in Hilbert space \mathbb{C}^m such that $\sum_i |x_i|^2 = 1$. We follow the Dirac bra/ket notation on quantum states, i.e., we denote the quantum state for \mathbf{x} by $|\mathbf{x}\rangle$ and denote \mathbf{x}^\dagger by $\langle \mathbf{x}|$, where \dagger means the Hermitian conjugation. Given a state $|\mathbf{x}\rangle = \sum_{i=1}^m x_i |i\rangle$, we

call x_i the amplitude of the state $|i\rangle$. Given two quantum states $|\mathbf{x}\rangle \in \mathbb{C}^m$ and $|\mathbf{y}\rangle \in \mathbb{C}^m$, we denote their inner product by $\langle \mathbf{x} | \mathbf{y} \rangle := \sum_i x_i^\dagger y_i$. Given $|\mathbf{x}\rangle \in \mathbb{C}^n$ and $|\mathbf{y}\rangle \in \mathbb{C}^m$, their tensor product is defined as $|\mathbf{x}\rangle \otimes |\mathbf{y}\rangle := (x_1 y_1, \dots, x_1 y_m, \dots, x_n y_1, \dots, x_n y_m)^\top$. A quantum algorithm works by applying a sequence of unitary operators to an input quantum state. In many cases, the quantum algorithms may have access to input data via unitary operators called *quantum oracles*. This operator can be accessed multiple times by a quantum algorithm. Hence, the *quantum query complexity* of a quantum algorithm is defined as the number of a quantum oracle being used. See (Nielsen and Chuang 2010) for detailed introductions to quantum computing.

Quantum Noisy Function Oracle. Our quantum non-linear bandit optimization setting follows that of the quantum multi-armed bandits in (Wan et al. 2023). In the quantum realm, each input \mathbf{x} is associated with a quantum sampling oracle. This oracle follows quantum sampling oracle (see appendix) and encodes the distribution of the corresponding noisy function value. More formally, let $Y_{\mathbf{x}}$ be the random variable of the noisy function value with input \mathbf{x} , and let $\Omega_{\mathbf{x}}$ be the finite sample space of this distribution. Then the sampling oracle for the noisy function value with input \mathbf{x} is defined as:

$$\mathcal{O}_{\mathbf{x}} : |\mathbf{0}\rangle \rightarrow \sum_{y \in \Omega_{\mathbf{x}}} \sqrt{\Pr[Y_{\mathbf{x}} = y]} |y\rangle \otimes |\psi_y\rangle, \quad (1)$$

where $|\psi_y\rangle$ is an arbitrary quantum state for each y . More detailed discussions on the justification of quantum oracles' feasibility and the relationships between them and their classical counterparts can be found in appendix.

Quantum Mean Estimation. For estimating the mean of an unknown distribution, we will use the following quantum Monte Carlo mean estimator as in (Wan et al. 2023; Wu et al. 2023; Dai et al. 2023):

Lemma 1 (Quantum Monte Carlo mean estimator (Montanaro 2015)). *Given the access to a quantum sampling oracle $\mathcal{O}_{\mathcal{Y}}$ (and its inverse $\mathcal{O}_{\mathcal{Y}}^\dagger$) that encodes the distribution of a random variable Y , as defined in Eq. (1).*

(1) **Bounded value:** *If the value of Y is taken from the interval $[0, 1]$, then there exists a constant $C_1 > 1$ a quantum algorithm $\text{QME}_1(\mathcal{O}_{\mathcal{Y}}, \epsilon, \delta)$ which returns an estimate \hat{y} such that with probability at least $1 - \delta$, $|\hat{y} - \mathbf{E}[Y]| \leq \epsilon$, using at most $\frac{C_1}{\epsilon} \log(1/\delta)$ queries to $\mathcal{O}_{\mathcal{Y}}$ and its inverse.*

(2) **Bounded variance:** *If $\text{Var}[Y] \leq \sigma^2$, then for $\epsilon < 4\sigma$, there is a constant $C_2 > 1$ and a quantum algorithm $\text{QME}_2(\mathcal{O}_{\mathcal{Y}}, \epsilon, \delta)$ which returns an estimate \hat{y} such that with probability at least $1 - \delta$, $|\hat{y} - \mathbf{E}[Y]| \leq \epsilon$, using at most $\frac{C_2 \sigma}{\epsilon} \log^{3/2}(8\sigma/\epsilon) \log(\log(8\sigma/\epsilon)) \log(1/\delta)$ queries to $\mathcal{O}_{\mathcal{Y}}$ and its inverse.*

As briefly discussed in (Wan et al. 2023), when aiming for a mean estimation error of ϵ , the QME algorithm achieves a quadratic reduction in query complexity compared to the classical one, which is crucial for the quantum speed-up in (Wan et al. 2023; Wu et al. 2023; Dai et al. 2023).

Assumptions

Assumption 2 (Realizable parametric function class). There exists an optimal $\mathbf{w}^* \in \mathcal{W}$ such that $f_0 = f_{\mathbf{w}^*}$. Also, w.l.o.g.,

$\mathcal{W} \subseteq [0, 1]^{d_w}$.

This assumption is commonly used in bandits (Foster and Rakhlin 2020; Simchi-Levi and Xu 2022) and reinforcement learning (Zhan et al. 2022; Zanette 2023). In Bayesian optimization (Srinivas et al. 2010; Chowdhury and Gopalan 2017), the RKHS assumption essentially assumes that the objective function is realizable within a certain RKHS function class. The realizable assumption allows one not to handle the function in misspecified settings (Bogunovic and Krause 2021; Liu, Yin, and Wang 2023), which is beyond the scope of this paper. The second assumption is on the structure of parametric function $f_{\mathbf{w}}$.

Assumption 3 (Bounded, differentiable, and smooth function). There exist constants $C_f, C_g, C_h > 0$ such that $\forall \mathbf{x} \in \mathcal{X}, \forall \mathbf{w} \in \mathcal{W}$, it holds that $|f_{\mathbf{x}}(\mathbf{w})| \leq C_f, \|\nabla f_{\mathbf{x}}(\mathbf{w})\|_2 \leq C_g, \|\nabla^2 f_{\mathbf{x}}(\mathbf{w})\|_{\text{op}} \leq C_h$.

This is a common assumption used in many non-convex optimization works (Kohler and Lucchi 2017; Li et al. 2023). Note it only puts mild structure conditions on the smoothness of parametric function $f_{\mathbf{w}}$ w.r.t. its parameter \mathbf{w} , rather than input \mathbf{x} , and the objective function f_0 can still be a black-box function of \mathbf{x} . The last assumption is on the expected loss function over uniform distribution \mathcal{U} .

Assumption 4 (Geometric conditions of loss function (Liu and Wang 2023)). $L(\mathbf{w}) = \mathbf{E}_{\mathbf{x} \sim \mathcal{U}}(f_{\mathbf{x}}(\mathbf{w}) - f_{\mathbf{x}}(\mathbf{w}^*))^2$ satisfies (τ, γ) -growth condition or μ -local strong convexity at \mathbf{w}^* , i.e., $\forall \mathbf{w} \in \mathcal{W}$,

$$\min \left\{ \frac{\mu}{2} \|\mathbf{w} - \mathbf{w}^*\|_2^2, \frac{\tau}{2} \|\mathbf{w} - \mathbf{w}^*\|_2^\gamma \right\} \leq L(\mathbf{w}) - L(\mathbf{w}^*),$$

for constants $\mu, \tau > 0, \mu < d_w$ and $0 < \gamma < 2$. Also, $L(\mathbf{w})$ satisfies a c -local self-concordance assumption at \mathbf{w}^* .

This assumption is needed for technical reasons in analyzing quantum regression oracle. Note the loss function $L(\mathbf{w})$ can be a highly non-convex function since it only assumes *local* strong convexity in the neighboring region of \mathbf{w}^* , strictly weaker than the global strong convexity, and growth condition when \mathbf{w} is away from \mathbf{w}^* . Careful readers are referred to Figure 1 in (Liu and Wang 2023) for a non-convex function example satisfying this assumption.

Q-NLB-UCB Algorithm

In this section, we show full details of the Q-NLB-UCB algorithm (Algorithm 1). First, in Step 1, we take a subroutine Algorithm 2 to query the quantum regression oracle QNLRO for T_0 times, which aims at solving the following non-linear regression problem to get an estimated parameter $\hat{\mathbf{w}}_0 \leftarrow \arg \min_{\mathbf{w} \in \mathcal{W}} \sum_{j=1}^{T_0} (f_0(\mathbf{x}_j) - y_j)^2$. Our goal is to make sure that $\hat{\mathbf{w}}_0$ satisfies

$$\|\hat{\mathbf{w}}_0 - \mathbf{w}^*\|_2 \leq \frac{C_0}{T_0}, \quad (2)$$

where C_0 denotes a constant. Careful readers may have noticed that in the classical (non-quantum) regime, the best upper bound is only $\|\hat{\mathbf{w}}_0 - \mathbf{w}^*\|_2 \leq O(1/\sqrt{T_0})$, which can be obtained using the small variance property of squared losses near optimal solution and applying the Craig-Bernstein (CB)

Algorithm 1 Q-NLB-UCB

Input: Objective function f_0 , initial covariance matrix $\Sigma_0 = \lambda \mathbf{I}$, quantum non-linear regression oracle QNLRO, regularization weight λ , confidence sequence β_s , constant C_1 .

- 1: $\hat{\mathbf{w}}_0 \leftarrow \text{QNLRO}(f_0, T_0, \delta/4)$
- 2: **for** each stage $s = 1, 2, \dots$ **do**
- 3: Update Σ_s by Eq. (3).
- 4: Update $\hat{\mathbf{w}}_s$ by Eq. (4).
- 5: Update Ball_s by Eq. (5).
- 6: Select $\mathbf{x}_s = \arg \max_{\mathbf{x} \in \mathcal{X}} \max_{\mathbf{w} \in \text{Ball}_s} f_{\mathbf{x}}(\mathbf{w})$.
- 7: Update $\epsilon_s = \|\nabla f_{\mathbf{x}_s}(\hat{\mathbf{w}}_0)\|_{\Sigma_s^{-1}}$.
- 8: **for** the next $\frac{C_1}{\epsilon_s} \log \frac{m}{\delta}$ rounds **do**
- 9: Take actions \mathbf{x}_s and run $\text{QME}_1(O_{\mathbf{x}_s}, \epsilon_s, \delta/m)$.
- 10: Obtain y_s as an estimation of $f_0(\mathbf{x}_s)$.
- 11: **end for**
- 12: **end for**

Output: $\hat{\mathbf{x}} \sim \mathcal{U}(\{\mathbf{x}_1, \dots, \mathbf{x}_T\})$.

Algorithm 2 Quantum Non-Linear Regression Oracle (QNLRO)

Input: Objective function f_0 , time T_0 , failure parameter $\delta \in [0, 1/2]$, quantum regression oracle Oracle.

- 1: $|\hat{\mathbf{w}}_0\rangle \leftarrow \text{Oracle}(f_0, T_0, \delta/4)$
- 2: **for** $i = 1, \dots, d_w$ **do**
- 3: set projector $P_i = |i\rangle\langle i|$
- 4: obtain $\tilde{a}_i \leftarrow \text{NDAE}(|\hat{\mathbf{w}}_0\rangle, P_i, \frac{1}{d_w \cdot T_0}, \frac{\delta}{4d_w})$
- 5: **end for**

Output: $\hat{\mathbf{w}}_0 = (\tilde{a}_1, \dots, \tilde{a}_{d_w})$.

inequality (Craig 1933). How can we achieve the quadratic improvement in quantum case? In short, we work with the quantum fast-forward technique (Apers and Sarlette 2019) and refine the analysis with the CB inequality. This gives the desirable convergence rate, but the parameter vector $\hat{\mathbf{w}}_0$ is returned in the form of a quantum state. To use it in classical state later, necessary techniques for retrieving the classical information of all the entries in $\hat{\mathbf{w}}_0$ will be employed. Specifically, we use *non-destructive amplitude estimation* (NDAE) (Rall and Fuller 2023). More details on techniques and analyses are given in the next section and full proofs are shown in appendix.

From Step 2 to Step 12, the algorithm runs in m stages where multiple rounds are conducted in each stage. Why doesn't it run in simply T rounds like classical bandit optimization? This design is due to the quantum Monte Carlo mean estimation (Lemma 1) where the same action needs to be taken multiple times. And we set $\epsilon_s = \|\nabla f_{\mathbf{x}_s}(\hat{\mathbf{w}}_0)\|_{\Sigma_s^{-1}}$ and $m = d_w \log \left(\frac{C_g^2 T^2}{d_w \lambda} + 1 \right)$ (Lemma 13) to ensure the total number of rounds is T . In addition to using QME_1 in Algorithm 1, our algorithm also works with QME_2 which is the bounded variance case in Lemma 1. The analysis will be similar to that of QME_1 .

Specifically in each stage $s = 1, \dots, m$, in Step 3, we construct the covariance matrix Σ_s by

$$\Sigma_s = \Sigma_{s-1} + \frac{1}{\epsilon_{s-1}^2} \nabla f_{\mathbf{x}_{s-1}}(\hat{\mathbf{w}}_0) \nabla f_{\mathbf{x}_{s-1}}(\hat{\mathbf{w}}_0)^\top, \quad (3)$$

where the $1/\epsilon_{s-1}^2$ is the weight assigned to query in each stage. Note here $\nabla f_{\mathbf{x}_{s-1}}(\hat{\mathbf{w}}_0)$ is the gradient of the parametric function f taken w.r.t. $\hat{\mathbf{w}}_0$, which can be easily obtained, and the objective function f_0 can still be a black-box function without any derivative information. Different from (Liu and Wang 2023), $\nabla f_{\mathbf{x}_{s-1}}(\hat{\mathbf{w}}_0)$ is not taken w.r.t. the fixed $\hat{\mathbf{w}}_{s-1}$ to save the tedious inductive argument in it while still doing the rank-1 updates since the action \mathbf{x}_{s-1} changes over stages. And the rank-1 updates are needed because the algorithm can save all historical information and add only one new matrix at each stage, according to Eq. (3). Then we define the following regression problem to estimate $\hat{\mathbf{w}}_s$:

$$\begin{aligned} \hat{\mathbf{w}}_s = \arg \min_{\mathbf{w}} & \frac{\lambda}{2} \|\mathbf{w} - \hat{\mathbf{w}}_0\|_2^2 \\ & + \frac{1}{2} \sum_{i=0}^{s-1} \frac{1}{\epsilon_i^2} \left((\mathbf{w} - \hat{\mathbf{w}}_0)^\top \nabla f_{\mathbf{x}_i}(\hat{\mathbf{w}}_0) + f_{\mathbf{x}_i}(\hat{\mathbf{w}}_0) - y_i \right)^2. \end{aligned} \quad (4)$$

Note in the first term $\|\mathbf{w} - \hat{\mathbf{w}}_0\|_2^2$, the regression center is set to be $\hat{\mathbf{w}}_0$ so that we can take advantage of Eq. (2) to reach a much faster convergence rate than constant as in QLinUCB (Wan et al. 2023). The design of the second term is using the first order Taylor expansion of parametric function $f_{\mathbf{x}_i}$ to approximate the noisy observation y_i . Solution to optimization problem in Eq. (4), $\hat{\mathbf{w}}_s$, further serves as the center of the parameter uncertainty region Ball_s , defined as

$$\text{Ball}_s = \{ \mathbf{w} \in \mathbb{R}^d : \|\mathbf{w} - \hat{\mathbf{w}}_s\|_{\Sigma_s}^2 \leq \beta_s \}. \quad (5)$$

The key design of Ball_s is to contain the optimal parameter \mathbf{w}^* in each stage s w.h.p., so that Q-NLB-UCB can keep track of \mathbf{w}^* at all times. The radius parameter β_s plays an important role in this design and later in Lemma 14 our confidence analysis shows that it suffices to choose β_s as

$$\beta_s = 3d_w s + \frac{3\lambda C_0^2}{T_0^2} + \frac{3C_h^2 C_0^2 s T^2}{4T_0^4}. \quad (6)$$

In Step 6, the choice of \mathbf{x}_s is generated by solving a cross optimization problem defined in both \mathcal{X} and Ball_s . While the exact solution of this step is hard to find, in practice one can use gradient ascent as a surrogate solution, and it works well in our experiments. The final output $\hat{\mathbf{x}}$ is uniformly sampled from all historical actions $\mathbf{x}_1, \dots, \mathbf{x}_T$ since $f^* - \mathbf{E}f(\hat{\mathbf{x}}) \leq R_T/T$, i.e., one can easily obtain the theoretical guarantee of $\hat{\mathbf{x}}$ using cumulative regret bound with uniform sampling. But in practice, one can also select \mathbf{x}_T as the output.

Theoretical Analysis

In this section, we provide theoretical analysis for Q-NLB-UCB. First, we analyze the quantum regression oracle that outputs $\hat{\mathbf{w}}_0$ to start the algorithm, then we provide the regret analysis to prove its input dimension-free $O(\text{poly log } T)$ regret bound, supported by the confidence analysis. Full proofs and time complexity analysis are deferred to appendix.

Quantum Non-Linear Regression Oracle

Here we show the existence of a quantum non-linear regression oracle which outputs the estimated parameter $\hat{\mathbf{w}}_0$ that satisfies Eq. (2). This algorithm involves two primary procedures: (1) obtaining a quantum state that encodes $\hat{\mathbf{w}}_0$; (2) retrieving the classical information of all entries in $\hat{\mathbf{w}}_0$. Roughly speaking, this result can be achieved by ‘‘quantizing’’ the proof of Theorem 5.2 in (Liu and Wang 2023) with quantum fast-forward technique (Apers and Sarlette 2019), shown below.

Lemma 5 (Adapted from Theorem 5.2 in (Liu and Wang 2023)). *Suppose Assumptions 2, 3, and 4 hold. There is an absolute value C such that after T_0 iterations in step 1 of Algorithm 1 where T_0 satisfies $T_0 \geq Cd_{\mathbf{w}}\iota \max \left\{ \frac{\mu^{\gamma/(2-\gamma)}}{\tau^{2/(2-\gamma)}}, \frac{2C_g^2}{\mu c^2} \right\}$, with probability $1 - \delta/2$, the quantum regression oracle returns an estimate $\hat{\mathbf{w}}_0$ that satisfies $\|\hat{\mathbf{w}}_0 - \mathbf{w}^*\|_2 \leq \sqrt{\frac{Cd_{\mathbf{w}}\iota}{T_0}}$, where ι is the logarithmic term depending on $T_0, C_h, 1/\delta$.*

Note that this lemma still gives $O(1/\sqrt{T_0})$ asymptotical rate after T_0 iterations, the same as in classical setting. To attain the desired faster $O(1/T_0)$ rate, we apply the quantum fast-forward technique introduced in (Apers and Sarlette 2019). An informal description below follows that in (Ambainis et al. 2020).

Lemma 6 (Informal statement of quantum fast-forward (Ambainis et al. 2020)). *Let $\epsilon \in (0, 1)$, $s \in [0, 1]$ and $t \in \mathbb{N}$. Given a reversible Markov chain determined by a matrix \mathbf{D} , there is a quantum algorithm with $O(\sqrt{t} \log(1/\epsilon))$ quantum walk steps that takes input $|\bar{0}\rangle|\psi\rangle \in \text{span}\{|\bar{0}\rangle|x\rangle : x \in X\}$, and outputs a state that is ϵ -close to a state of the form $|0\rangle^{\otimes a}|\bar{0}\rangle D^t|\psi\rangle + |\Gamma\rangle$ where $a = O(\log(t \log(1/\epsilon)))$, $|\bar{0}\rangle$ is some fixed reference state, and $|\Gamma\rangle$ is some garbage state that has no support on states containing $|0\rangle^{\otimes a}|\bar{0}\rangle$ in the first two registers.*

Consequently, we can summarize the goal of Step 1 in Algorithm 1 with the following theorem. Full proofs are deferred to appendix.

Theorem 7. *Suppose Assumptions 2, 3, and 4 hold. There is an absolute value C such that after $\tilde{O}(T_0)$ iterations in step 1 of Algorithm 2 where T_0 satisfies $T_0^2 \geq Cd_{\mathbf{w}}\iota \max \left\{ \frac{\mu^{\gamma/(2-\gamma)}}{\tau^{2/(2-\gamma)}}, \frac{2C_g^2}{\mu c^2} \right\}$ with probability $1 - \delta/2$, the quantum regression oracle returns a quantum state that encodes an estimate $\hat{\mathbf{w}}_0$ that satisfies $\|\hat{\mathbf{w}}_0 - \mathbf{w}^*\|_2 \leq \sqrt{\frac{Cd_{\mathbf{w}}\iota}{T_0}}$, where ι is the logarithmic term depending on $T_0, C_h, 1/\delta$.*

So far we have proved the convergence of information provided by $|\hat{\mathbf{w}}_0\rangle$. This means that after applying the quantum regression oracle, we will be returned with a quantum state $|\hat{\mathbf{w}}_0\rangle$ which encodes the parameter vector $\hat{\mathbf{w}}_0$ that meets the convergence guarantee. Next for the classical usage of parameter vector $\hat{\mathbf{w}}_0$, we need to retrieve them from the quantum state $|\hat{\mathbf{w}}_0\rangle$. A standard approach will be employing quantum state tomography. But this will be an overkill because in general quantum state tomography considers the cases where the $\log N$ -qubit quantum state input to be in \mathbf{C}^N . Recall that with loss of generality, our work focuses on $|\hat{\mathbf{w}}_0\rangle \in [0, 1]^{d_w}$.

Hence, we can employ a more efficient tool, named *quantum amplitude estimation*, which outputs an estimate of $\langle \psi | P | \psi \rangle$ upon input a quantum state $|\psi\rangle$ and a projector P . However, the execution of straight quantum amplitude estimation algorithm will cause the input state $|\psi\rangle$ to collapse, which means $O(\text{poly}(d_w, \epsilon, \delta))$ many copies of the input quantum states are needed for gaining the classical information of all the entries in $|\psi\rangle$. In our problem, this preparation of multiple copies of the state $|\hat{\mathbf{w}}_0\rangle$ will require queries to the quantum sampling oracles \mathcal{O}_x , thus dramatically increasing the cumulative regret, which is undesirable. That means that our problem lies in scenarios where $|\psi\rangle$ is extremely expensive to prepare. To avoid this, we turn to *non-destructive amplitude estimation* which can return an estimation of $\langle \psi | P | \psi \rangle$ and also give the copy of $|\psi\rangle$ back. There are multiple existing works in this field. (Rall and Fuller 2023) listed multiple of them and we pick one among them. An informal description is stated below.

Theorem 8 ((Informal) Non-destructive amplitude estimation in (Rall and Fuller 2023)). *Given one copy of a quantum state $|\psi\rangle$, a projector P , and $\epsilon, \delta \in [0, 1/2]$. Let $a = \langle \psi | P | \psi \rangle$. Then there is an algorithm NDAE($|\psi\rangle, P, \epsilon, \delta$) that with probability at least $1 - \delta$, outputs an estimate \tilde{a} and a copy of $|\psi\rangle$ such that $|\tilde{a} - a| \leq \epsilon$.*

Let **Oracle** denote a quantum algorithm that solves the non-linear regression problem and outputs a quantum state encoding the solution that satisfies the convergence bound provided by Theorem 7. Combining Theorem 7 and Theorem 8, we obtain the following result for the quantum non-linear regression oracle (QNLRO, Algorithm 2).

Theorem 9. *Suppose Assumptions 2, 3, and 4 hold. Then Algorithm 2 returns with probability $1 - \delta/2$, a classical vector of an estimate $\hat{\mathbf{w}}_0$ that satisfies $\|\hat{\mathbf{w}}_0 - \mathbf{w}^*\|_2 \leq \frac{\sqrt{C}d_w\iota}{T_0}$, where ι is the logarithmic term depending on $T_0, C_h, 1/\delta$ and T_0 satisfies $T_0^2 \geq Cd_w\iota \max\left\{\frac{\mu^\gamma/(2-\gamma)}{\tau^{2/(2-\gamma)}}, \frac{2C_g^2}{\mu c^2}\right\}$.*

The above theorem implies that it is sufficient to use only one copy of $|\hat{\mathbf{w}}_0\rangle$ to extract the classical information of all of its entries, given the fact that all the entries belong to $[0, 1]$. More concretely, Algorithm 2 first calls a quantum algorithm Oracle to obtain a quantum state that has the solution parameter vector. Then it uses NDAE with projectors that project onto each computational basis, i.e. $\langle \hat{\mathbf{w}}_0 | i \rangle \langle i | \hat{\mathbf{w}}_0 \rangle$, to retrieve each entry, respectively. Note that each time NDAE returns not only an estimate of an entry but also a copy of the original $|\hat{\mathbf{w}}_0\rangle$. Additionally, since NDAE doesn't query the sampling oracle \mathcal{O}_x , its execution incurs no extra cumulative regret.

Regret Analysis

Now we present the cumulative regret bound of our proposed Q-NLB-UCB algorithm.

Theorem 10 (Cumulative regret bound of Q-NLB-UCB). *Suppose Assumptions 2, 3, and 4 hold. There is an absolute value C such that after $\tilde{O}(T_0)$ iterations in Step 1 of Algorithm 1 where T_0 satisfies $T_0^2 \geq Cd_w\iota \max\left\{\frac{\mu^\gamma/(2-\gamma)}{\tau^{2/(2-\gamma)}}, \frac{2C_g^2}{\mu c^2}\right\}$ with ι denoting a logarithmic*

term depending on $T_0, C_h, 1/\delta$. Then Algorithm 1 with parameters $T_0 = \sqrt{T}, \lambda = T$ satisfies that with probability at least $1 - \delta$, $R_T = O(d_w^2 \log^{\frac{3}{2}}(T) \log(d_w \log(T)))$.

Remark 11. Note d_w is the parameter complexity of f_w , which is *not* necessarily related to the input dimension d_x of f_0 , therefore, our regret bound is input dimension-free. In practice, d_w can be smaller or larger than d_x since d_w solely depends on the users' choice of parametric functions, which can be linear or quadratic functions, or even deep neural networks. When f_w is chosen to be a linear function, our algorithm reduces back to the linear bandits as in QLinUCB (Wan et al. 2023). Compared with Q-GP-UCB (Dai et al. 2023) and QMCKernelUCB (Hikima et al. 2024), our algorithm takes a different technical route to successfully avoid the curse of dimensionality limitation. Moreover, our bound is at the $\log^{\frac{3}{2}}(T) \log \log T$ rate, which is also faster than classical lower bound $\Omega(\sqrt{T})$, showing the power of quantum computing.

Remark 12. The choices of $T_0 = \sqrt{T}, \lambda = T$ require careful analyses among quantum regression oracle, regret analysis, and confidence analysis. T_0 cannot be chosen too large to enforce a large T and it cannot be chosen too small to break the property of $\hat{\mathbf{w}}_0$ in Eq. (2). The choice of λ is obtained by balancing between different terms in regret analysis to ensure a poly log T -style bound.

Proof Sketch. The proof starts from the instantaneous regret in a single round in one stage. Since we are dealing with non-linear bandit optimization where the objective function is not necessarily linear, we use Taylor's theorem to expand the objective function into first order terms and high-order terms. The first order terms are handled like linear bandits (Wan et al. 2023), but the remaining high-order terms are bounded creatively using the convex property of parameter uncertainty region Ball_s multiple times. After we obtain the upper bound for a single round in one stage, we multiply it by number of rounds in one stage and obtain the bound for one stage. Later, we prove the following lemma to show the total number of stages in Q-NLB-UCB to make sure the total number of rounds is T .

Lemma 13 (Number of stages). *The Algorithm 1 runs at most $m = d_w \log\left(\frac{C_g^2 T^2}{d_w \lambda} + 1\right)$ stages.*

Note again in this lemma, d_w is the dimension of parameters, rather than d_x . This is because we are using $\nabla f_{x_i}(\hat{\mathbf{w}}_0)$ as the feature vector and its dimension is d_w . After proving Lemma 13, we take the summation of upper bounds and reach the upper bound of cumulative regret.

Confidence Analysis

The previous regret builds upon the successful construction of the confidence ball Ball_s for each stage s , which is summarized in the following confidence analysis lemma.

Lemma 14 (Confidence bound of Q-NLB-UCB). *Suppose Assumptions 2, 3, and 4 hold and β_s is chosen as Eq. (6). Then with parameters $T_0 = \sqrt{T}, \lambda = T$ in each stage s in Algorithm 1, the optimal parameter \mathbf{w}^* is trapped in*

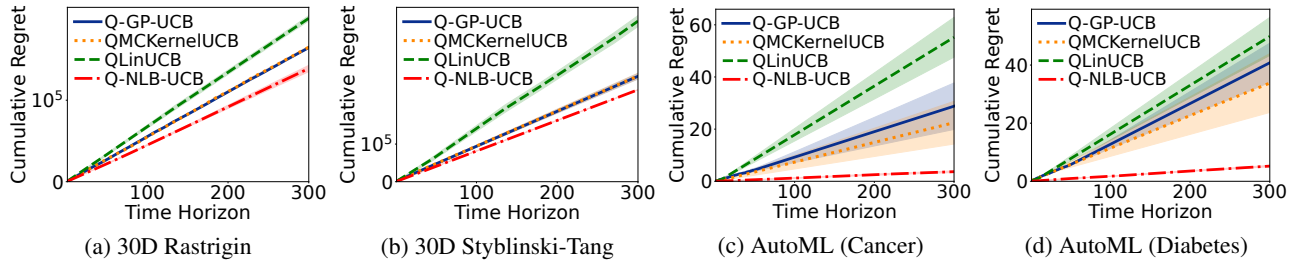


Figure 1: Cumulative regrets (the lower the better) of all compared quantum bandit algorithms.

confidence ball Ball_s with probability at least $1 - \delta$, i.e., $\|\hat{\mathbf{w}}_s - \mathbf{w}^*\|_{\Sigma_s}^2 \leq \beta_s$.

Remark 15. The design of Ball_s is similar to that in LinUCB (Abbasi-Yadkori, Pál, and Szepesvári 2011) and QLinUCB (Wan et al. 2023), but our choice of β_s is different. β_s cannot be too small to lose the track of optimal parameter \mathbf{w}^* and it cannot be too large as it appears in final regret bound. Overall the confidence analysis ensures that $\beta_s = \tilde{O}(1)$ and slightly grows as the stage index s .

Experiments

Experimental Setup. We compare the performance of our Q-NLB-UCB algorithm with QLinUCB (Wan et al. 2023), Q-GP-UCB (Dai et al. 2023) and QMCKernelUCB (Hikima et al. 2024). According to (Hikima et al. 2024), the only difference between Q-GP-UCB and QMCKernelUCB is a trade-off parameter η balancing the precision of quantum amplitude estimation and the noise in observations, and when $\eta = 1$, they become the same. In our experiments, we set $\eta = 0.1$ for QMCKernelUCB. To run Q-NLB-UCB, we set our parametric function model $f_{\mathbf{w}}$ to be a two linear layer neural network with the sigmoid activation function. Our implementation is based upon the sklearn, BoTorch (Balandat et al. 2020), and Qiskit (Javadi-Abhari et al. 2024). To stay consistent with theoretical analysis, cumulative regret is also used to evaluate algorithms. In order to reduce the impact of randomness in algorithms, we repeat each experiment 5 times and report the mean and adjusted standard errors of cumulative regrets, i.e., $\text{mean} \pm \text{std}/\sqrt{5}$.

High-Dimensional Synthetic Functions. We test all four algorithms on two functions, Rastrigin function and Styblinski-Tang function, defined in 30-dimensional space $[-5, 5]^{30}$. Q-NLB-UCB performs well as evidenced in Figure 1(a)(b), where it consistently achieves the lowest cumulative regret across multiple runs, outperforming all other algorithms. It is not a surprise as Q-GP-UCB and QMCKernelUCB suffer from the curse of dimensionality and Q-GP-UCB was only tested in 1-d and 2-d settings in (Dai et al. 2023). QLinUCB performs the worst since it is designed to work on linear functions only while both two test functions here are highly non-linear.

In addition, we report the runtime of three quantum bandit algorithms in seconds shown in Table 1. Among the three algorithms, our Q-NLB-UCB algorithm achieves a significantly low runtime, which again shows the efficiency of Q-NLB-UCB and validates our theoretical time complexity

Algorithms	Rastrigin	Styblinski-Tang
Q-GP-UCB	4629.6453	4139.2478
QMCKernelUCB	3744.1179	2565.0690
Q-NLB-UCB (ours)	861.2402	919.7602

Table 1: Runtime (in seconds) on two synthetic functions

analysis in appendix. We don’t list the runtime of QLinUCB because it is a linear bandit algorithm running faster but not comparable to algorithms designed for non-linear optimization.

Real-World AutoML Tasks. We test all four quantum bandit algorithms on three different hyperparameter tuning tasks for Support Vector Machine (SVM), Multi-Layer Perceptron (MLP), and Gradient Boosting (GB). We are tuning 4 hyperparameters in SVM, 8 in MLP, and 11 for GB. Each classifier is trained by different hyperparameter configurations and the goal is to maximize the validation accuracy on a hold-out set. Due to page limit, we only show results of MLP in Figure 1(c)(d) on both breast cancer and diabetes datasets, and readers are referred to appendix for similar results of SVM and GB. Again our Q-NLB-UCB algorithm outperforms all other algorithms by achieving significantly smaller regrets, demonstrating its strong potential for practical applications.

Conclusion

With the aid of quantum computing, recent works (Dai et al. 2023; Hikima et al. 2024) showed that new $O(\text{poly} \log T)$ regret bound can be achieved in quantum non-linear bandit optimization, but their works heavily rely on the RKHS assumption which suffers from the curse of dimensionality. Real-world data usually sit in high-dimensional spaces, making their regret bounds vacuous. In this paper, we develop the new Q-NLB-UCB algorithm which efficiently solves the problem in high-dimensional cases. The key design of Q-NLB-UCB involves quantum Monte Carlo mean estimation, parametric function approximation, and quantum fast-forward techniques, which all contribute to the new *input dimension-free* regret bound of Q-NLB-UCB. Moreover, the choice of parametric functions can be generic, such as linear or quadratic functions, or even deep neural networks. Technically, our analysis of the new quantum non-linear regression oracle can be of independent interests in more quantum machine learning problems in the future.

Acknowledgments

The authors would like to thank the anonymous reviewers for helpful comments that improved the final version of this paper.

References

- Abbasi-Yadkori, Y.; Pál, D.; and Szepesvári, C. 2011. Improved algorithms for linear stochastic bandits. *NIPS*, 24.
- Allen-Zhu, Z. 2018. Katyusha: The first direct acceleration of stochastic gradient methods. *JMLR*, 18(221): 1–51.
- Ambainis, A.; Gilyén, A.; Jeffery, S.; and Kokainis, M. 2020. Quadratic speedup for finding marked vertices by quantum walks. In *STOC*.
- Apeldoorn, J. v.; and Gilyén, A. 2018. Improvements in Quantum SDP-Solving with Applications. In *ICALP*.
- Apers, S.; and Sarlette, A. 2019. Quantum fast-forwarding: Markov chains and graph property testing. *Quantum Information and Computation*, 19(3–4): 181–213.
- Balandat, M.; Karrer, B.; Jiang, D.; Daulton, S.; Letham, B.; Wilson, A. G.; and Bakshy, E. 2020. BoTorch: A framework for efficient Monte-Carlo Bayesian optimization. *NeurIPS*, 33.
- Bogunovic, I.; and Krause, A. 2021. Misspecified gaussian process bandit optimization. *NeurIPS*, 34.
- Brandão, F. G. S. L.; and Svore, K. M. 2017. Quantum Speed-Ups for Solving Semidefinite Programs. In *FOCS*.
- Casares, P. A. M.; and Martin-Delgado, M. A. 2020. A quantum interior-point predictor–corrector algorithm for linear programming. *Journal of Physics A: Mathematical and Theoretical*, 53(44): 445305.
- Chakrabarti, S.; Childs, A. M.; Li, T.; and Wu, X. 2020. Quantum algorithms and lower bounds for convex optimization. *Quantum*, 4: 221.
- Chen, Z.; Lu, Y.; Wang, H.; Liu, Y.; and Li, T. 2025. Quantum Langevin Dynamics for Optimization. *Communications in Mathematical Physics*, 406(3): 52.
- Childs, A. M.; Leng, J.; Li, T.; Liu, J.-P.; and Zhang, C. 2022. Quantum simulation of real-space dynamics. *Quantum*, 6: 860.
- Chowdhury, S. R.; and Gopalan, A. 2017. On kernelized multi-armed bandits. In *ICML*.
- Clarke, R.; Ransom, H. W.; Wang, A.; Xuan, J.; Liu, M. C.; Gehan, E. A.; and Wang, Y. 2008. The properties of high-dimensional data spaces: implications for exploring gene and protein expression data. *Nature Reviews Cancer*, 8(1): 37–49.
- Craig, C. C. 1933. On the Tchebycheff inequality of Bernstein. *The Annals of Mathematical Statistics*, 4(2): 94–102.
- Dai, Z.; Lau, G. K. R.; Verma, A.; Shu, Y.; Low, B. K. H.; and Jaillet, P. 2023. Quantum bayesian optimization. *NeurIPS*, 36.
- Dai, Z.; Shu, Y.; Low, B. K. H.; and Jaillet, P. 2022. Sample-then-optimize batch neural Thompson sampling. *NeurIPS*, 35.
- Diaconis, P.; and Miclo, L. 2013. On the spectral analysis of second-order Markov chains. *Annales de la Faculté des sciences de Toulouse: Mathématiques*, 22(3): 573–621.
- Fang, C.; Li, C. J.; Lin, Z.; and Zhang, T. 2018. Spider: Near-optimal non-convex optimization via stochastic path-integrated differential estimator. *NIPS*, 31.
- Foster, D.; and Rakhlin, A. 2020. Beyond ucb: Optimal and efficient contextual bandits with regression oracles. In *ICML*.
- Frazier, P. I. 2018. A tutorial on Bayesian optimization. *arXiv preprint arXiv:1807.02811*.
- Frazier, P. I.; and Wang, J. 2016. Bayesian optimization for materials design. *Information science for materials discovery and design*, 45–75.
- Garg, A.; Kothari, R.; Netrapalli, P.; and Sherif, S. 2021a. Near-optimal lower bounds for convex optimization for all orders of smoothness. *NeurIPS*, 34.
- Garg, A.; Kothari, R.; Netrapalli, P.; and Sherif, S. 2021b. No Quantum Speedup over Gradient Descent for Non-Smooth Convex Optimization. In *Innovations in Theoretical Computer Science Conference*.
- Gong, W.; Zhang, C.; and Li, T. 2025. Robustness of Quantum Algorithms for Nonconvex Optimization. In *ICLR*.
- He, J.; Liu, C.; Liu, X.; Li, L.; and Lui, J. C. 2024. Quantum algorithm for online exp-concave optimization. In *Proceedings of the 41st International Conference on Machine Learning*, 17946–17971.
- He, J.; Yang, F.; Zhang, J.; and Li, L. 2022. Quantum algorithm for online convex optimization. *Quantum Science and Technology*, 7(2): 025022.
- Hikima, Y.; Murao, K.; Takemori, S.; and Umeda, Y. 2024. Quantum Kernelized Bandits. In *UAI*.
- Javadi-Abhari, A.; Treinish, M.; Krsulich, K.; Wood, C. J.; Lishman, J.; Gacon, J.; Martiel, S.; Nation, P. D.; Bishop, L. S.; Cross, A. W.; et al. 2024. Quantum computing with Qiskit. *arXiv preprint arXiv:2405.08810*.
- Jones, D. R.; Schonlau, M.; and Welch, W. J. 1998. Efficient global optimization of expensive black-box functions. *Journal of Global optimization*, 13: 455–492.
- Kandasamy, K.; Neiswanger, W.; Schneider, J.; Póczos, B.; and Xing, E. P. 2018. Neural architecture search with bayesian optimisation and optimal transport. *NIPS*, 31.
- Kerenidis, I.; and Prakash, A. 2020. A quantum interior point method for LPs and SDPs. *ACM Transactions on Quantum Computing*, 1(1): 1–32.
- Kohler, J. M.; and Lucchi, A. 2017. Sub-sampled cubic regularization for non-convex optimization. In *ICML*.
- Korovina, K.; Xu, S.; Kandasamy, K.; Neiswanger, W.; Póczos, B.; Schneider, J.; and Xing, E. 2020. Chembo: Bayesian optimization of small organic molecules with synthesizable recommendations. In *AISTATS*.
- Leng, J.; Hickman, E.; Li, J.; and Wu, X. 2023. Quantum hamiltonian descent. *arXiv preprint arXiv:2303.01471*.
- Li, H.; Qian, J.; Tian, Y.; Rakhlin, A.; and Jadbabaie, A. 2023. Convex and non-convex optimization under generalized smoothness. *NeurIPS*, 36.

- Li, T.; and Zhang, R. 2022. Quantum speedups of optimizing approximately convex functions with applications to logarithmic regret stochastic convex bandits. *NeurIPS*, 35.
- Liu, C.; Guan, C.; He, J.; and Lui, J. C. 2024. Quantum Algorithms for Non-smooth Non-convex Optimization. *NeurIPS*, 37.
- Liu, C.; and Wang, Y.-X. 2023. Global optimization with parametric function approximation. In *ICML*.
- Liu, C.; Yin, M.; and Wang, Y.-X. 2023. No-regret linear bandits beyond realizability. In *UAI*.
- Liu, Y.; Su, W. J.; and Li, T. 2023. On quantum speedups for nonconvex optimization via quantum tunneling walks. *Quantum*, 7: 1030.
- Montanaro, A. 2015. Quantum speedup of Monte Carlo methods. *Proceedings of the Royal Society A: Mathematical, Physical and Engineering Sciences*, 471(2181): 1–20.
- Nielsen, M. A.; and Chuang, I. L. 2010. *Quantum computation and quantum information*. Cambridge university press.
- Nowak, R. 2009. Lecture notes: Complexity regularization for squared error loss.
- Rahnenführer, J.; De Bin, R.; Benner, A.; Ambrogio, F.; Lusa, L.; Boulesteix, A.-L.; Migliavacca, E.; Binder, H.; Michiels, S.; Sauerbrei, W.; et al. 2023. Statistical analysis of high-dimensional biomedical data: a gentle introduction to analytical goals, common approaches and challenges. *BMC Medicine*, 21(1): 182.
- Rall, P.; and Fuller, B. 2023. Amplitude estimation from quantum signal processing. *Quantum*, 7: 937.
- Russo, D. J.; Van Roy, B.; Kazerouni, A.; Osband, I.; Wen, Z.; et al. 2018. *A tutorial on thompson sampling*. now publishers.
- Scarlett, J.; Bogunovic, I.; and Cevher, V. 2017. Lower bounds on regret for noisy gaussian process bandit optimization. In *COLT*.
- Scott, W.; Frazier, P.; and Powell, W. 2011. The correlated knowledge gradient for simulation optimization of continuous parameters using gaussian process regression. *SIAM Journal on Optimization*, 21(3): 996–1026.
- Sidford, A.; and Zhang, C. 2023. Quantum speedups for stochastic optimization. *NeurIPS*, 36.
- Simchi-Levi, D.; and Xu, Y. 2022. Bypassing the monster: A faster and simpler optimal algorithm for contextual bandits under realizability. *Mathematics of Operations Research*, 47(3): 1904–1931.
- Snoek, J.; Rippel, O.; Swersky, K.; Kiros, R.; Satish, N.; Sundaram, N.; Patwary, M.; Prabhat, M.; and Adams, R. 2015. Scalable bayesian optimization using deep neural networks. In *ICML*.
- Springenberg, J. T.; Klein, A.; Falkner, S.; and Hutter, F. 2016. Bayesian optimization with robust Bayesian neural networks. *NIPS*, 29.
- Srinivas, N.; Krause, A.; Kakade, S.; and Seeger, M. 2010. Gaussian Process Optimization in the Bandit Setting: No Regret and Experimental Design. In *ICML*.
- van Apeldoorn, J.; Gilyén, A.; Gribling, S.; and de Wolf, R. 2020. Convex optimization using quantum oracles. *Quantum*, 4: 220.
- Wan, Z.; Zhang, Z.; Li, T.; Zhang, J.; and Sun, X. 2023. Quantum multi-armed bandits and stochastic linear bandits enjoy logarithmic regrets. In *AAAI*.
- Wang, Y.; Balakrishnan, S.; and Singh, A. 2019. Optimization of smooth functions with noisy observations: Local minimax rates. *IEEE Transactions on Information Theory*, 65(11): 7350–7366.
- Williams, C. K.; and Rasmussen, C. E. 2006. *Gaussian processes for machine learning*. MIT press Cambridge, MA.
- Wu, J.; Toscano-Palmerin, S.; Frazier, P. I.; and Wilson, A. G. 2020. Practical multi-fidelity Bayesian optimization for hyperparameter tuning. In *UAI*.
- Wu, Y.; Guan, C.; Aggarwal, V.; and Wang, D. 2023. Quantum heavy-tailed bandits. *arXiv preprint arXiv:2301.09680*.
- Zanette, A. 2023. When is realizability sufficient for off-policy reinforcement learning? In *ICML*.
- Zhan, W.; Huang, B.; Huang, A.; Jiang, N.; and Lee, J. 2022. Offline reinforcement learning with realizability and single-policy concentrability. In *COLT*.
- Zhang, C.; Leng, J.; and Li, T. 2021. Quantum algorithms for escaping from saddle points. *Quantum*, 5: 529.
- Zhang, C.; and Li, T. 2023. Quantum lower bounds for finding stationary points of nonconvex functions. In *ICML*.
- Zhang, W.; Zhou, D.; Li, L.; and Gu, Q. 2021. Neural Thompson Sampling. In *ICLR*.
- Zhang, Y.; Zhang, C.; Fang, C.; Wang, L.; and Li, T. 2024. Quantum Algorithms and Lower Bounds for Finite-Sum Optimization. In *ICML*.
- Zhou, D.; Li, L.; and Gu, Q. 2020. Neural contextual bandits with ucb-based exploration. In *ICML*.

Auxiliary Lemmas

In this section, we show auxiliary lemmas and definitions that will be used later in proofs.

Lemma 16 (Upper bound of summation of weights (Adapted from Lemma 2 in (Dai et al. 2023))). *Set $\epsilon_s = \|\nabla f_{\mathbf{x}_s}(\hat{\mathbf{w}}_0)\|_{\Sigma_s^{-1}}$, then it satisfies that*

$$\sum_{s=1}^m \frac{1}{\epsilon_s} \leq T \quad \text{and} \quad \sum_{s=1}^m \frac{1}{\epsilon_s^2} \leq T^2.$$

Proof. First we can lower bound the total number of rounds in m stages. Following Eq. (9), we have

$$\sum_{s=1}^m \frac{C_1}{\epsilon_s} \log \frac{m}{\delta} \geq \sum_{s=1}^m \frac{1}{\epsilon_s} \geq \sqrt{\sum_{s=1}^m \frac{1}{\epsilon_s^2}}.$$

Suppose that $\sum_{s=1}^m \frac{1}{\epsilon_s^2} \geq T^2$, then we have

$$\sum_{s=1}^m \frac{C_1}{\epsilon_s} \log \frac{m}{\delta} > T,$$

which is a contradiction. Similarly we can prove both statements. □

Lemma 17 (Wainwright (2019)). *Let X be a random variable with mean μ and variance σ^2 . If X satisfies the following Bernstein moment condition,*

$$\mathbf{E}[|X - \mu|^k] \leq \frac{\sigma^2}{2} k! \beta^{k-2}$$

for some $\beta > 0$ and all $k \geq 2$, then

$$\mathbf{E}[e^{\lambda(X-\mu)}] \leq \exp\left(\frac{\lambda^2 \sigma^2}{2(1-\beta\lambda)}\right), \quad \forall \lambda \in \left[0, \frac{1}{\beta}\right).$$

Discussion on Quantum Oracle

Quantum Access to Random Variables. Unlike classical access to samples of random variables, in quantum realm, the corresponding distribution is being accessed by making query to quantum sampling oracle.

Definition 18 (Quantum sampling oracle). For a random variable Y with (finite) sample space Ω , its quantum sampling oracle \mathcal{O}_Y is defined as

$$\mathcal{O}_Y : |0\rangle \mapsto \sum_{\mathbf{y} \in \Omega} \sqrt{\Pr[Y = \mathbf{y}]} |\mathbf{y}\rangle \otimes |\psi_{\mathbf{y}}\rangle, \quad (7)$$

where $|\psi_{\mathbf{y}}\rangle$ is an arbitrary quantum state for every \mathbf{y} .

The content in second quantum register can also be viewed as possible quantum garbage appeared during the implementation of the oracle. Observe that if we directly measure the output of \mathcal{O}_Y , it will collapse to a classical sampling access to Y that returns a random sample \mathbf{y} with respect to probability $\Pr[Y = \mathbf{y}]$. In particular, the quantum noisy function Eq. (1) is an instance of the quantum sampling oracle.

Feasibility and Practicality. This same type of quantum oracles were also used in previous work (Wan et al. 2023; Dai et al. 2023; Hikima et al. 2024; Sidford and Zhang 2023). As discussed in (Dai et al. 2023), a quantum oracle is available when the learning environment is implemented by a quantum algorithm, which makes the setting of their quantum Bayesian optimization fairly general. Therefore, for example, such quantum oracles will arise naturally when quantum bandit algorithms are used to optimize hyperparameters of quantum neural networks and any other quantum machine learning models. Furthermore, there are standard techniques (Nielsen and Chuang 2010) in theory for implementing the quantum analogs of classical algorithms. Specifically, if there is a classical circuit for the given classical oracle, its quantum version of the same asymptotic computational complexity can be built using standard technique. Thus, in some scenarios, quantum oracles can be considered as a quantum generalization of their classical counterparts, and then this framework can be applied to optimize the parameters of models implemented on a quantum computer or in quantum systems where the data itself is inherently quantum, as pointed out in (Dai et al. 2023). In particular, (Dai et al. 2023) successfully implemented their algorithm in the IBM real quantum computer, which shows that the quantum oracle can be fully realized in the real world.

In practice, however, the current development of quantum hardware is still at a relatively early stage. The actual implementation feasibility depends on factors such as circuit size and the complexity of the required quantum gates. Therefore, we believe that our quantum oracle can be practically feasible in small-size problem settings where the oracle is given as an explicit circuit.

Full Proofs

In this section, we show full proofs of all technical results in the main paper.

Quantum Non-Linear Regression Oracle

In this section, we first review the details and properties for step 1 of Algorithm 2, and the rest of the algorithm. At the end we provide the necessary theoretical analysis for the complete Algorithm 2.

Proof Overview on Oracle In this section, we describe the quantum regression oracle, denoted as Oracle in step 1 in Algorithm 2, that we need for solving a non-linear *non-linear least square* problem.

Let $D^{T_0} \mathbf{w}$ denote a classical algorithm for solving a *non-linear least square* problem where \mathbf{w} is an initial value of the solution and D is a matrix representing one iteration of the algorithm. It is easy to see that Markov chain-based algorithms (e.g SGD) can be represented using this notation.

Before presenting the actual proof of Theorem 7, we provide a high-level overview of the key technical aspects. The core idea in proving Lemma 5.1 is formulating the difference between expected risk and empirical risk as bounded variables satisfying a certain condition and then applying the Craig-Bernstein (CB) inequality (Craig 1933). In the formulation, the variable is linked to the unknown parametric function within the optimization problem (i.e. $f_{\mathbf{w}}(\mathbf{x})$), and the inequality is then utilized in a summation across a set of data samples. This approach is standard for classical algorithms. However, to fully harness the quantum advantage, we can employ a quantum sampling oracle on the dataset, as defined in Eq. (7). With such oracle, the random variables being used in the proof will be associated with the expected risk function $L(\mathbf{w})$, and then the summation in the application of CB inequality will be computed over the the number of iterations. Note that this approach still only yields a rate of $\tilde{O}(1/T_0)$. To obtain an improved rate of $\tilde{O}(1/T_0^2)$, we leverage the quadratic speed-up provided by quantum computing when implementing algorithms that satisfy the framework specified as in $D^{T_0} \mathbf{w}$. While such quantum enhancements can be realized using quantum singular value transformation (Gilyén et al. 2019), we instead adopt the quantum fast-forward technique introduced in (Apers and Sarlette 2019), following the description in (Ambainis et al. 2020).

Theorem 19 (Formal rephrase of Theorem 6 in (Ambainis et al. 2020)). *Let $\epsilon \in (0, 1)$, $s \in [0, 1]$ and $t \in \mathbb{N}$. Let P be any transition matrix which defines a reversible Markov chain on state space X and D be its discriminant matrix. Also let Q be the cost of implementing a quantum walk step. There is a quantum algorithm with complexity $O(Q\sqrt{t \log(1/\epsilon)})$ that takes input $|\bar{0}\rangle|\psi\rangle \in \text{span}\{|\bar{0}\rangle|x\rangle : x \in X\}$, and outputs a state that is ϵ -close to a state of the form*

$$|0\rangle^{\otimes a} |\bar{0}\rangle D^t |\psi\rangle + |\Gamma\rangle \quad (8)$$

where $a = O(\log(t \log(1/\epsilon)))$, $|\bar{0}\rangle$ is some fixed reference state, and $|\Gamma\rangle$ is some garbage state that has no support on states containing $|0\rangle^{\otimes a} |\bar{0}\rangle$ in the first two registers.

Informally, this theorem shows that a t -step classical random walk/Markov chain can be closely approximated by quantum walk using only \sqrt{t} steps. This implies that the same performance guarantees achieved by a t -step classical random walk can also be attained by a quantum algorithm with time complexity $\propto \sqrt{t}$.

A more visual intuition on how the step 1 of Algorithm 1 works is pictured in Figure 2. It describes a high-level picture of a quantum algorithm implementing $D^{T_0} \mathbf{w}$ which denotes an execution of a classical algorithm solving a non-linear least square problem. More concretely, the input qubits to the quantum algorithm can be divided into three different parts: parameter register, input data register, and auxiliary qubits. Then the complete quantum process before the measurement step gives $(UL)^{T_0} |w\rangle |0\rangle |0\rangle$ (here 0's in the last two registers can represent multiple qubits), and the resulting state will have information of $D^{T_0} \mathbf{w}$. The composite operator UL makes one step of the quantum walk, like one update in SGD. During each step, operator L transforms the input from the last step into a quantum state whose expected value yields the gradient, and U performs the update process.

In quantum algorithms leveraging Markov chains for optimization problems, their inputs can be decomposed into three parts. The parameter register consists of qubits that store the parameter information. The input data register is dedicated to generating the distribution for data samples. The auxiliary qubits provide the workspace for temporary information produced during the quantum algorithms that are not part of the final output. Given an input state across those three registers, the quantum oracle \mathcal{L} —whose detailed description will be discussed in the subsequent paragraph—transforms the input into a quantum state whose expectation value yields the gradient $\nabla \mathcal{L}$. While techniques from (Sidford and Zhang 2023) enable unbiased mean estimation for gradient extraction, we omit further details here as they lie outside our scope. The unitary \mathbf{U} then processes the output of \mathcal{L} , implementing a single iteration of a Markov-chain-based update rule, say determined by \mathbf{D} , for solving non-linear least square problems. Roughly speaking, \mathbf{U} combines two components: (1) an unbiased non-destructive multivariate mean estimation subroutine; and (2) a quantum walk step over the parameter space. The composite operation $\mathbf{U}\mathcal{L}$ constitutes one full iteration of the algorithm, as formalized in Theorem 19. Starting from the initial state, after T_0 iterations, i.e. $(\mathbf{U}\mathcal{L})^{T_0} |\mathbf{w}\rangle |0\rangle |0\rangle$, the final quantum state will encodes $\mathbf{D}^{T_0} \mathbf{w}$. To gain a quadratic speed-up, we apply the quantum fast-forward technique to $(\mathbf{U}\mathcal{L})^{T_0}$. Consequently, the step 1 of Algorithm 1 approximates Eq. (8) with $\tilde{O}(\sqrt{T_0})$ iterations.

Since the quantum oracle \mathcal{L} plays a pivotal role in the process, we now give a detailed discussion of its implementation requirements and constraints. To formalize its purpose, without loss of generality, consider the gradient of loss function

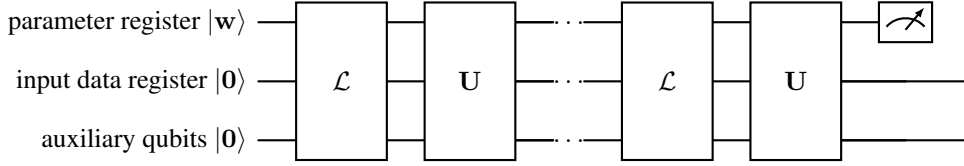


Figure 2: High-level description of a quantum algorithm computing $D^{T_0} \mathbf{w}$

$\mathbf{E}_{\mathbf{x} \sim D}[(f_{\mathbf{w}}(\mathbf{x}) - f_{\mathbf{w}^*}(\mathbf{x}))^2]$, where the parametric function f can be viewed as a function with input (\mathbf{w}, \mathbf{x}) . By standard differentiation, its gradient is $\mathbf{E}_{\mathbf{x} \sim D}[2(f_{\mathbf{w}}(\mathbf{x}) - f_{\mathbf{w}^*}(\mathbf{x})) \nabla f_{\mathbf{w}}(\mathbf{x})]$. The oracle \mathcal{L} must therefore prepare a quantum state whose expectation value encodes this gradient. Note that \mathcal{L} viewed as an operator maps $|\mathbf{w}\rangle$ to a quantum state $\sum_Y \sqrt{\Pr[Y]} |\mathcal{A}(Y)\rangle$ for some operations \mathcal{A} , and its expectation gives $\mathbf{E}_Y[\mathcal{A}(Y)]$. Hence, we need to design the necessary \mathcal{A} so that the multivariate mean value $\mathbf{E}_Y[\mathcal{A}(Y)]$ produces $\mathbf{E}_{\mathbf{x} \sim D}[2(f_{\mathbf{w}}(\mathbf{x}) - f_{\mathbf{w}^*}(\mathbf{x})) \nabla f_{\mathbf{w}}(\mathbf{x})]$. One caveat is that $f_{\mathbf{w}^*}(\mathbf{x})$ is not accessible directly. Instead, we are given access to the quantum noisy function oracle Eq. (1). However, this limitation can be addressed by leveraging the fact that $\mathbf{E}[y] = f_{\mathbf{w}^*}(\mathbf{x})$. Overall, we can construct the quantum oracle \mathcal{L} as follows.

Given the quantum noisy function oracle $\mathcal{O}_{\mathbf{x}}$ (as defined in Eq. (1)) for all \mathbf{x} in \mathcal{X} , we can obtain the following quantum oracle \mathcal{L} :

$$\mathcal{L} : |\mathbf{w}\rangle|0\rangle|0\rangle \mapsto \sum_{\mathbf{x}} \sum_{\mathbf{e}} \sqrt{\Pr[\mathbf{x}]} \cdot \sqrt{\Pr[\mathbf{e}]} (f_{\mathbf{w}}(\mathbf{x}) - (f_{\mathbf{w}^*}(\mathbf{x}) + \mathbf{e})) \cdot \frac{\partial f_{\mathbf{w}}(\mathbf{x})}{\partial w_1} \rangle \otimes \cdots \otimes (f_{\mathbf{w}}(\mathbf{x}) - (f_{\mathbf{w}^*}(\mathbf{x}) + \mathbf{e})) \cdot \frac{\partial f_{\mathbf{w}}(\mathbf{x})}{\partial w_d} \rangle \otimes |\text{garbage}\rangle.$$

The proof for this conversion is straightforward. By standard quantum computation principles, any classical circuit g can be embedded into a quantum circuit G such that: $|\mathbf{x}\rangle|0\rangle \xrightarrow{G} |\mathbf{x}\rangle|g(\mathbf{x})\rangle$. Building on this, without loss of generality, we construct a quantum circuit that prepares a quantum state whose expectation value encodes the gradient of expected loss function $L = \mathbf{E}_{\mathbf{x}}[(f_{\mathbf{x}}(\mathbf{w}) - f_{\mathbf{x}}(\mathbf{w}^*))^2]$. Three components enable this: (1) the parametric function f is classically specified; (2) the data input distribution can be created from scratch efficiently; and (3) the value $f_{\mathbf{x}}(\mathbf{w}^*)$ can be obtained as the mean of the operator in Eq. (1). Following the standard embedding process mentioned above, these three components are combined into a unified quantum circuit acting on registers.

Overview on Algorithm 2 Let $|\hat{\mathbf{w}}_0\rangle$ be the quantum state returned by Oracle in step 1 and write $|\hat{\mathbf{w}}_0\rangle = \sum_i^{d_{\mathbf{w}}} a_i |i\rangle$. The rest of Algorithm 2 is about retrieving a_i 's for $i = 1, \dots, d_{\mathbf{w}}$. One standard approach to achieve that is using quantum state tomography. However, in our case, we can use amplitude estimation instead because each $a_i \in [0, 1]$. At the same we want to avoid repeatedly calling Oracle for obtaining more copies of $|\hat{\mathbf{w}}_0\rangle$ since that will dramatically increase the number of queries to the quantum sampling oracle $\mathcal{O}_{\mathbf{x}}$, which will in turn cause extra cumulative regret. Hence, we will a technique called *non-destructive amplitude estimation* which can return both an estimate of a_i and a copy of the input state $|\hat{\mathbf{w}}_0\rangle$. There are multiple existing works in this field. (Rall and Fuller 2023) listed multiple of them and we pick one among them. Below is a more formal statement of Theorem 8.

Theorem 20 (Non-destructive amplitude estimation in (Rall and Fuller 2023)). *Given one copy of a quantum state $|\psi\rangle$, a projector P , and $\epsilon, \delta \in [0, 1/2]$. Let $a = \langle \psi | P | \psi \rangle$. Then there is a quantum algorithm NDAE($|\psi\rangle, P, \epsilon, \delta$) that outputs with probability at least $1 - \delta$, an estimate \tilde{a} and a copy of $|\psi\rangle$ such that $|\tilde{a} - a| \leq \epsilon$ and it uses the reflections and rotations on $|\psi\rangle$ and P $\tilde{O}(\frac{1}{\epsilon\sqrt{\delta}})$ times.*

Remark 21. Given a projector P , its reflection can be defined as $2P - I$ or $I - 2P$, and its rotation is defined as $e^{2\theta(2P - I)}$ or $e^{2\theta(I - 2P)}$ for arbitrary phases θ . Note that the projector for a quantum state $|\psi\rangle$ can be represented as $|\psi\rangle\langle\psi|$. Hence, the reflections and rotations for state $|\psi\rangle$ can be defined similarly. Since neither reflections or rotations require queries to the quantum sampling oracles $\mathcal{O}_{\mathbf{s}}$, the usage of them will not contribute to cumulative regret. Hence, their implementations are outside the scope of our work. Interested readers can refer to (Rall and Fuller 2023) for details on how to implement them using the given state and projector.

With NDAE, we can retrieve an estimate for each a_i for $i = 1, \dots, d_{\mathbf{w}}$ with only one copy of $|\hat{\mathbf{w}}_0\rangle$, thus avoiding the expenses caused by repeatedly solving a non-linear least square problem. Overall, the correctness of Algorithm 2 is a result of Theorem 7 and Theorem 20, which can be summarized as follows.

Theorem 22 (Restatement of Theorem 9). *Suppose Assumptions 2, 3, and 4 hold. Then Algorithm 2 returns with probability $1 - \delta/2$, a classical vector of an estimate $\hat{\mathbf{w}}_0$ that satisfies*

$$\|\hat{\mathbf{w}}_0 - \mathbf{w}^*\|_2 \leq \frac{\sqrt{C d_{\mathbf{w}} t}}{T_0},$$

where ι is the logarithmic term depending on $T_0, C_h, 1/\delta$ and T_0 satisfies $T_0^2 \geq Cd_{\mathbf{w}}\iota \max\left\{\frac{\mu^{\gamma/(2-\gamma)}}{\tau^{2/(2-\gamma)}}, \frac{2C_g^2}{\mu c^2}\right\}$.

Its proof is presented in the next section.

Theoretical Analysis Recall that a quantum sampling oracle enables the access to a superposition that entirely encodes a distribution of finite size. The following notations will be found convenient in constructing our proofs. Let $Y(Z) = f_{\mathbf{w}^*}(Z)$ and define $F_{\mathbf{w}}(X) := \sum_{Z \in D(X)} (f_{\mathbf{w}}(Z) - Y(Z))^2 = \sum_{i=1}^M (f_{\mathbf{w}}(Z_i) - Y(Z))^2$ where $D(X)$ is some probability distribution with finite sample space $\Omega \subseteq \mathbf{R}^d$ centered at X of size $|\Omega| = M$, $L(f_{\mathbf{w}}) = \mathbf{E}_X F_{\mathbf{w}}(X)$, and $\hat{L}(f_{\mathbf{w}}) = 1/T_0 \sum_{i=1}^{T_0} F_{\mathbf{w}}(X_i)$. It is easy to check that $\mathbf{E}_X[\hat{L}(f_{\mathbf{w}})] = L(f_{\mathbf{w}})$. We also assume that the output value of f is contained in a interval of length $b \geq 1$. Note that if $M = 1$, then the quantum sampling oracle becomes a classical oracle. Hence, without loss of generality, we can have $M \gg 1$.

Remark 23. In classical setting, $Y(Z) = f_{\mathbf{w}^*}(Z) + \eta$, and a $Y(Z)$ is returned when querying with input Z , and one can estimate $f_{\mathbf{w}^*}(Z)$ by Chernoff bound. However, in quantum realm, one can extract $f_{\mathbf{w}^*}(Z)$ while still maintaining it as a quantum superposition instead of a classical sample by mean estimation algorithms (Montanaro 2015; Sidford and Zhang 2023) without performing the measurement. Therefore, it is not a strong relaxation to have $Y(Z) = f_{\mathbf{w}^*}(Z)$ in the analysis.

Lemma 24. *Given an oracle that accesses a dataset $\{Z, f_{\mathbf{w}^*}(Z)\}_{Z \in D(X)}$ where D is some distribution with finite sample space $\Omega \subseteq \mathbf{R}^d$ centered at X when queried with input X . Let \mathcal{F} be a finite function class satisfying $\mathcal{F} \subset \{f : [0, 1]^d \rightarrow [-b, b]\}$ for some $b \geq 1$ and define empirical risk minimizer (ERM) $\hat{f}_{T_0} := \arg \min_{f \in \mathcal{F}} \{\hat{L}(f)\}$. Then with probability at least $1 - \delta$, the following holds*

$$L(\hat{f}_{T_0}) \leq \frac{1 + \alpha}{1 - \alpha} L(\tilde{f}) + 2 \frac{\log |\mathcal{F}| + \log 2/\delta}{(1 - \alpha)T_0\epsilon}$$

where $\epsilon < \frac{c_1^{k/(k-2)}}{4Lb^2}$, $\alpha = \epsilon b^2$, and $\tilde{f} \in \mathcal{F}$ is arbitrary.

Proof. The proof follows a structure similar to that in (Nowak 2009), but some extra work is needed for our application. Define variables $U_i = -F_{\mathbf{w}}(X_i)$. Then $L(f_{\mathbf{w}}) - \hat{L}(f_{\mathbf{w}}) = \frac{1}{T_0} \sum_{i=1}^{T_0} (U_i - \mathbf{E}_X[U_i])$. In order to apply the CB inequality (Craig 1933) as in (Nowak 2009), we need to (1) verify that the variables U_i satisfy the Bernstein's moment condition

$$\mathbf{E}_{X_i} [|U_i - \mathbf{E}_{X_i}[U_i]|^k] \leq \frac{\text{Var}[U_i]}{2} k! h^{k-2}$$

for some $h > 0$ and all $k \geq 2$; (2) find an upper bound for $\text{Var}[U_i]$. They can be achieved by the following two claims.

Claim 25. The Bernstein's moment condition holds with $h = \frac{2\sqrt{Mb}}{c_1}$ with some constant c_1 where $1 \leq c_1 < \sqrt{\text{Var}[U]}/\beta$, $\sqrt{\text{Var}[U]} \neq c_1\beta$, and $\beta = \frac{2b^2}{3}$.

Claim 26.

$$\text{Var}[U_i] \leq b^2 L(F_{\mathbf{w}}).$$

Suppose Theorem 25 and Theorem 26 hold. By applying the CB inequality with certain values ϵ and c , which will be determined later, we obtain that, with probability at least $1 - \delta$,

$$L(f_{\mathbf{w}}) - \hat{L}(f_{\mathbf{w}}) \leq \frac{\log 1/\delta}{T_0\epsilon} + \frac{\epsilon b^2 L(F_{\mathbf{w}})}{2(1 - c)}$$

for $0 < \epsilon h \leq c < 1$. Following the Kraft inequality and union bound trick on the finite set \mathcal{F} in (Nowak 2009), we have that, for any $\delta > 0$,

$$L(f_{\mathbf{w}}) - \hat{L}(f_{\mathbf{w}}) \leq \frac{\log |\mathcal{F}| + \log 1/\delta}{T_0\epsilon} + \frac{\epsilon b^2 L(f_{\mathbf{w}})}{2(1 - c)}, \quad \forall f_{\mathbf{w}} \in \mathcal{F}$$

with probability at least $1 - \delta$.

Claim 27. Let $0 < \epsilon < \frac{c_1}{4Mb^2}$, $c = \epsilon h$, and $\alpha = \epsilon b^2$. Then $0 < c < \frac{1}{2}$ and $\frac{\epsilon b^2}{2(1 - c)} < \alpha < 1$.

By Theorem 27, we rearrange to get

$$(1 - \alpha)L(f_{\mathbf{w}}) \leq \hat{L}(f_{\mathbf{w}}) + \frac{\log |\mathcal{F}| + \log 1/\delta}{T_0\epsilon}, \quad \forall f_{\mathbf{w}} \in \mathcal{F}$$

with probability at least $1 - \delta$. Define

$$\hat{f}_{T_0} := \arg \min_{f_{\mathbf{w}} \in \mathcal{F}} \{\hat{L}(f_{\mathbf{w}})\}.$$

Then with probability at least $1 - \delta$,

$$\begin{aligned} (1 - \alpha)L(\hat{f}_{T_0}) &\leq \hat{L}(\hat{f}_{T_0}) + \frac{\log |\mathcal{F}| + \log 1/\delta}{T_0\epsilon}, \\ &\leq \hat{L}(\tilde{f}) + \frac{\log |\mathcal{F}| + \log 1/\delta}{T_0\epsilon}, \end{aligned}$$

where $\tilde{f} \in \mathcal{F}$ is arbitrary. Similarly, we apply CB inequality to $\hat{L}(\tilde{f}) - L(\tilde{f}) = \frac{1}{T_0} \sum_{i=1}^{T_0} -(U_i - \mathbf{E}_X[U_i])$ and attain

$$\hat{L}(\tilde{f}) - L(\tilde{f}) \leq \alpha L(\tilde{f}) + \frac{\log |\mathcal{F}| + \log 1/\delta}{T_0\epsilon}$$

with probability at least $1 - \delta$. By union bound, we get

$$L(\hat{f}_{T_0}) \leq \frac{1 + \alpha}{1 - \alpha} L(\tilde{f}) + 2 \frac{\log |\mathcal{F}| + \log 1/\delta}{(1 - \alpha)T_0\epsilon}$$

with probability at least $1 - 2\delta$, for any $\delta > 0$. \square

Lemma 28. *Suppose Theorem 2 and Theorem 3 hold. There is an absolute constant C' , such that after T_0 iterations in Step 1 of Algorithm 1, with probability at least $1 - \delta/2$, the quantum regression oracle returns an estimate $\hat{\mathbf{w}}_0$ that satisfies*

$$L(f_{\hat{\mathbf{w}}_0}) \leq \frac{C' d_{\mathbf{w}} \iota}{T_0},$$

where ι is a logarithmic term depending on $T_0, C_h, 1/\delta$.

Proof. Its proof follows that of Lemma 5.1 in (Liu and Wang 2023) with minor changes. We provide it here for completeness.

Let $\tilde{\mathbf{w}}, \tilde{\mathcal{W}}$ denote the ERM parameter and finite parameter class after applying covering number argument on \mathcal{W} . By Theorem 24, we obtain that with probability at least $1 - \delta/2$,

$$\begin{aligned} L(f_{\tilde{\mathbf{w}}}) &\leq \frac{1 + \alpha}{1 - \alpha} L(f_{\mathbf{w}^*}) + 2 \frac{\log |\mathcal{F}| + \log 4/\delta}{(1 - \alpha)T_0\epsilon}, \\ &\leq 2 \frac{\log |\mathcal{F}| + \log 4/\delta}{(1 - \alpha)T_0\epsilon}, \end{aligned}$$

where the first inequality follows from $\mathbf{w}^* \in \tilde{\mathcal{W}} \cup \{\mathbf{w}^*\}$. Our parameter class $\mathcal{W} \subseteq [0, 1]^{d_{\mathbf{w}}}$, so by ϵ -covering number argument, $\log(|\tilde{\mathcal{W}}|) = \log(1/\epsilon'^{d_{\mathbf{w}}}) = d_{\mathbf{w}} \log(1/\epsilon')$, and then we have with probability at least $1 - \delta/2$,

$$L(f_{\tilde{\mathbf{w}}}) \leq C'' \frac{d_{\mathbf{w}} \log(1/\epsilon') + \log 4/\delta}{T_0},$$

where C'' is a universal constant determined by α and ϵ picked in Theorem 24. By $(a + b)^2 \leq 2a^2 + 2b^2$,

$$\begin{aligned} L(f_{\hat{\mathbf{w}}_0}) &\leq 2\mathbf{E}_X \left[\sum_{Z \in \mathcal{D}(X)} (f_{\hat{\mathbf{w}}_0}(Z) - f_{\tilde{\mathbf{w}}}(Z))^2 \right] + 2L(f_{\tilde{\mathbf{w}}}), \\ &\leq 2\epsilon'^2 C_h^2 + 2C'' \frac{d_{\mathbf{w}} \log(1/\epsilon') + \log 4/\delta}{T_0}, \end{aligned}$$

where the second inequality applies discretization error ϵ' and Theorem 3. By choosing $\epsilon' = \frac{1}{C_h \sqrt{T_0}}$, the bound above becomes

$$\frac{2}{T_0} + \frac{C'' d_{\mathbf{w}} \log(T_0 C_h^2)}{T_0} + \frac{2C'' \log 4/\delta}{T_0} \leq C' \frac{d_{\mathbf{w}} \log(T_0 C_h^2) + \log(4/\delta)}{T_0},$$

where we can take $C' = 2C''$ and assume $2 < C'' d_{\mathbf{w}} \log(T_0 C_h^2)$. The proof completes by defining ι as the logarithmic term depending on $T_0, C_h, 1/\delta$. \square

Lemma 29 (Restatement of Theorem 5). *Suppose Assumptions 2, 3, and 4 hold. There is an absolute value C such that after T_0 iterations in step 1 of Algorithm 1 where T_0 satisfies*

$$T_0 \geq C d_{\mathbf{w}} \iota \max \left\{ \frac{\mu^{\gamma/(2-\gamma)}}{\tau^{2/(2-\gamma)}}, \frac{2C_g^2}{\mu c^2} \right\},$$

with probability $1 - \delta/2$, the quantum regression oracle returns an estimate $\hat{\mathbf{w}}_0$ that satisfies

$$\|\hat{\mathbf{w}}_0 - \mathbf{w}^*\|_2 \leq \sqrt{\frac{C d_{\mathbf{w}} \iota}{T_0}},$$

where ι is the logarithmic term depending on $T_0, C_h, 1/\delta$.

Its proof follows that of Theorem 5.2 in (Liu and Wang 2023) with no changes required. Note that the rate of $\|\hat{\mathbf{w}}_0 - \mathbf{w}^*\|_2$ is still $\tilde{O}(1/\sqrt{T_0})$ after T_0 iterations. To achieve the same rate of $\tilde{O}(1/\sqrt{T_0})$ after $\sqrt{T_0}$ iterations, we turn to Theorem 19 which shows that the T_0 iterations can be approximately with only $\sqrt{T_0}$ iterations.

Theorem 30 (Restatement of Theorem 7). *Suppose Assumptions 2, 3, and 4 hold. There is an absolute value C such that after $\tilde{O}(T_0)$ iterations in step 1 of Algorithm 2 where T_0 satisfies*

$$T_0^2 \geq C d_{\mathbf{w}} \iota \max \left\{ \frac{\mu^{\gamma/(2-\gamma)}}{\tau^{2/(2-\gamma)}}, \frac{2C_g^2}{\mu c^2} \right\},$$

with probability $1 - \delta/2$, the quantum regression oracle returns an estimate $\hat{\mathbf{w}}_0$ that satisfies

$$\|\hat{\mathbf{w}}_0 - \mathbf{w}^*\|_2 \leq \frac{\sqrt{C d_{\mathbf{w}} \iota}}{T_0},$$

where ι is the logarithmic term depending on $T_0, C_h, 1/\delta$.

Proof. Suppose we select an algorithm used in this step following $D^{T_0} \mathbf{w}$. Let T_0 be the number of iterations in this algorithm. Then it can be formulated $D^{T_0} \mathbf{w}$ with a random initial parameter vector \mathbf{w} , and the estimate output $\hat{\mathbf{w}}_0 = D^{T_0} \mathbf{w}$. By Theorem 5, we obtain that with probability at least $1 - \delta/2$,

$$\|\hat{\mathbf{w}}_0 - \mathbf{w}^*\|_2^2 \leq \frac{C d_{\mathbf{w}} \iota}{T_0}$$

after T_0 iterations of exact calculation.

Next by Theorem 19, we have that there is a quantum algorithm \mathcal{A} can output a vector \mathbf{w}' that is $\sqrt{\epsilon_1}$ -close to $D^{T_0} \mathbf{w}$ with time complexity $O(Q\sqrt{T_0} \log(1/\sqrt{\epsilon_1}))$ where Q is the cost of performing one quantum walk step. That implies that with $O(\sqrt{T_0} \log(1/\sqrt{\epsilon_1}))$ iterations, \mathcal{A} will return an estimate $\sqrt{\epsilon_1}$ -close to $\hat{\mathbf{w}}_0$. Overall, there is a quantum algorithm that takes input a random initial parameter \mathbf{w} and outputs an estimate $\hat{\mathbf{w}}_0'$ such that with probability at least $1 - \delta/2$,

$$\|\hat{\mathbf{w}}_0' - \mathbf{w}^*\|_2^2 \leq \frac{C d_{\mathbf{w}} \iota}{T_0} + \epsilon_1$$

with $O(\sqrt{T_0} \log(1/\sqrt{\epsilon_1}))$ steps. Finally, the desired statement can be derived by setting $\epsilon_1 = 1/T_0$ and change of variable. \square

Proof for Theorem 22. Denote $|\hat{\mathbf{w}}_0\rangle = \sum_i^{d_{\mathbf{w}}} b_i |i\rangle$. It is easy to check that $\langle \hat{\mathbf{w}}_0 | P_i | \hat{\mathbf{w}}_0 \rangle$ gives $|b_i|^2$. Note that as a vector $\hat{\mathbf{w}}_0 \in [0, 1]^{d_{\mathbf{w}}}$, which means $|b_i| = b_i$.

Let $\delta' = \frac{\delta}{4d_{\mathbf{w}}}$. Then by Theorem 20, NDAE($|\hat{\mathbf{w}}_0\rangle, P_i, \frac{1}{d_{\mathbf{w}} T_0^2}, \delta'$) outputs with probability at least $1 - \delta'$, an estimate \tilde{a}_i of b_i^2 such that $|\tilde{a}_i - b_i^2| \leq \frac{1}{d_{\mathbf{w}} T_0^2}$. Since both $\sqrt{\tilde{a}_i}$ and b_i are nonnegative, we have

$$|\sqrt{\tilde{a}_i} - b_i| \leq \sqrt{|\tilde{a}_i - b_i^2|} \leq \frac{1}{\sqrt{d_{\mathbf{w}} \cdot T_0^2}}.$$

Let $\tilde{\mathbf{w}}_0 = (\sqrt{\tilde{a}_1}, \dots, \sqrt{\tilde{a}_{d_{\mathbf{w}}}})$. Then

$$\|\tilde{\mathbf{w}}_0 - \hat{\mathbf{w}}_0\|_2^2 = \sum_i^{d_{\mathbf{w}}} |\sqrt{\tilde{a}_i} - b_i|^2 \leq \frac{1}{T_0^2},$$

and by triangle inequality,

$$\|\tilde{\mathbf{w}}_0 - \mathbf{w}^*\|_2 \leq \|\tilde{\mathbf{w}}_0 - \hat{\mathbf{w}}_0\|_2 + \|\hat{\mathbf{w}}_0 - \mathbf{w}^*\|_2 \leq \frac{1 + \sqrt{C d_{\mathbf{w}} \iota}}{T_0}$$

where the last equality follows from the combination of the upper bound on $\|\tilde{\mathbf{w}}_0 - \hat{\mathbf{w}}_0\|_2$ and that on $\|\hat{\mathbf{w}}_0 - \mathbf{w}^*\|_2$ provided by Theorem 30.

Next, it is left to prove the success probability. First, step 1 in Algorithm 2 calls Oracle which has $\mathcal{O}(T_0)$ iterations and its success probability is at least $1 - \delta/4$. Second, each NDAE($|\hat{\mathbf{w}}_0\rangle, P_i, \frac{1}{d_{\mathbf{w}} T_0^2}, \delta'$) succeeds with probability at $1 - \delta'$. Hence, all the $d_{\mathbf{w}}$ calls to NDAE outputs the correct estimates with probability at least

$$(1 - \delta')^{d_{\mathbf{w}}} \geq 1 - d_{\mathbf{w}} \cdot \delta' = 1 - \frac{\delta}{4}$$

where the first equality follows from Bernoulli's inequality and the last step comes from the definition of δ' .

Overall, Algorithm 2 successfully outputs $\hat{\mathbf{w}}_0 = (\hat{a}_1, \dots, \hat{a}_{d_{\mathbf{w}}})$ with probability at least $(1 - \frac{\delta}{4})^2 \geq 1 - \frac{\delta}{2}$ as desired. \square

Proof of Theorem 25. For each independent random variable $Z_i \sim D(X)$, define random variable $J_i = -(f(Z_i|\mathbf{w}) - f(Z_i|\mathbf{w}^*))^2$ and $V_i = J_i - \mathbf{E}[J_i]$. Then we can see that $U = \sum_{Z_i \sim D(X)} J_i$ with $\text{Var}[J_i] \leq b^2$, and $\mathbf{E}[V_i] = 0$. Since $D(X)$ has finite sample space Ω of size $|\Omega| = M$, we write $U = \sum_{\ell=1}^M J_\ell$, and hence $\text{Var}[U] \leq Mb^2$.

Next let $W = U - \mathbf{E}[U] = \sum_{\ell=1}^M V_\ell$ and observe that $\mathbf{E}[W] = 0$. As in (Nowak 2009), note that each independent J_i satisfies the following Bernstein condition

$$\mathbf{E}[|J_i - \mathbf{E}[J_i]|^k] = \mathbf{E}[|V_i|^k] \leq \frac{\text{Var}[J_i]}{2} k! \beta^{k-2}$$

for all $k \geq 2$ and with $\beta = \frac{2b^2}{3}$. Then by Theorem 17, we have that for each J_i ,

$$\mathbf{E}[e^{\lambda V_i}] = \mathbf{E}[e^{\lambda(J_i - \mathbf{E}[J_i])}] \leq \exp\left(\frac{\lambda^2 \text{Var}[J_i]}{2(1 - \lambda\beta)}\right), \quad \forall \lambda \in \left[0, \frac{1}{\beta}\right].$$

Next we put all M independent V_i together to get, with the same λ ,

$$\mathbf{E}[e^{\lambda W}] = \mathbf{E}\left[\prod_{i=1}^M e^{\lambda V_i}\right] = \prod_{i=1}^M \mathbf{E}[e^{\lambda V_i}] \leq \exp\left(\frac{\lambda^2 \text{Var}[U]}{2(1 - \lambda\beta)}\right), \quad \forall \lambda \in \left[0, \frac{1}{\beta}\right].$$

Note that this also holds when replacing W with $-W$. Hence, for $m = 1, 2, \dots$

$$\frac{\lambda^{2m}}{(2m)!} \mathbf{E}[W^{2m}] \leq \mathbf{E}\left[\frac{e^{\lambda W} + e^{-\lambda W}}{2}\right] \leq \exp\left(\frac{\lambda^2 \text{Var}[U]}{2(1 - \lambda\beta)}\right),$$

where the first inequality follows from the Taylor series of exponential functions.

Next we let $\lambda = \frac{c_1}{\sqrt{\text{Var}[U]}}$ with some constant $c_1 \geq 1$ such that $\sqrt{\text{Var}[U]} \neq c_1\beta$ and $\lambda < 1/\beta$. Then we can verify that $\exp\left(\frac{\lambda^2 \text{Var}[U]}{2(1 - \lambda\beta)}\right)$ as a function of $\text{Var}[U]$ is decreasing for all $\text{Var}[U] \geq 0$ and $\sqrt{\text{Var}[U]} \neq c_1\beta$.

With substitution and rearrangement, we can derive

$$\mathbf{E}[W^{2m}] \leq (2m)! \frac{1}{\lambda^{2m}} \leq (2m)! \left(\frac{\sqrt{\text{Var}[U]}}{c_1}\right)^{2m}.$$

Next we apply Cauchy-Schwarz inequality to attain, for $m = 1, 2, \dots$,

$$\begin{aligned} \mathbf{E}[|W|^{2m+1}] &\leq \sqrt{\mathbf{E}[W^{2m}] \mathbf{E}[W^{2m+2}]}, \\ &\leq \sqrt{(2m)! \left(\frac{\sqrt{\text{Var}[U]}}{c_1}\right)^{2m} \sqrt{(2m+2)! \left(\frac{\sqrt{\text{Var}[U]}}{c_1}\right)^{2m+2}}}, \\ &\leq (2m+1)! \left(\frac{\sqrt{\text{Var}[U]}}{c_1}\right)^{2m+1}. \end{aligned}$$

Therefore, we have

$$\begin{aligned} \mathbf{E}[|U - \mathbf{E}[U]|^k] &= \mathbf{E}[|W|^k], \\ &\leq k! \left(\frac{\sqrt{\text{Var}[U]}}{c_1}\right)^k, \\ &\leq k! \frac{1}{c_1^k} \text{Var}[U] (\sqrt{\text{Var}[U]})^{k-2}, \\ &\leq \frac{\text{Var}[U]}{2} k! \frac{(2\sqrt{Mb})^{k-2}}{c_1^k}, \\ &\leq \frac{\text{Var}[U]}{2} k! \left(\frac{2\sqrt{Mb}}{c_1}\right)^{k-2}, \end{aligned}$$

where the last step follows from $c_1 \geq 1$. □

Proof of Theorem 26. By the definition of U_i , we have

$$U_i^2 = F_{\mathbf{w}}(X_i)^2,$$

$$\begin{aligned}
&= \sum_{\mathbf{Z}, \mathbf{Z}' \in \mathcal{D}(X)} (f_{\mathbf{w}}(\mathbf{Z}) - f_{\mathbf{w}^*}(\mathbf{Z}))^2 (f_{\mathbf{w}}(\mathbf{Z}') - f_{\mathbf{w}^*}(\mathbf{Z}'))^2, \\
&\leq b^2 \sum_{\mathbf{Z} \in \mathcal{D}(X)} (f_{\mathbf{w}}(\mathbf{Z}) - f_{\mathbf{w}^*}(\mathbf{Z}))^2,
\end{aligned}$$

and then

$$\text{Var}[U_i] \leq \mathbf{E}[U_i^2] = L(F_{\mathbf{w}}).$$

□

Proof of Theorem 27. When $\epsilon < \frac{c_1}{4Mb^2}$,

$$c = \epsilon h = \epsilon \frac{2\sqrt{Mb}}{c_1} < \frac{1}{2\sqrt{Mb}} < \frac{1}{2}$$

where the second step is by the value of h from Theorem 25 and the last step follows from the fact that $M, b \geq 1$.

Next,

$$\alpha = \epsilon b^2 < \frac{c_1}{4M}.$$

It is straightforward that $\alpha > \frac{\epsilon b^2}{2(1-c)}$ since $c > 0$. Note that by Theorem 25,

$$1 \leq c_1 < \frac{\sqrt{\text{Var}[U]}}{\beta} \leq \frac{3\sqrt{M}}{2b},$$

since $\sqrt{\text{Var}[U]} \leq \sqrt{Mb}$ and $\beta = 2b^2/3$. Then

$$\alpha < \frac{c_1}{4M} < \frac{3\sqrt{M}}{2b} \cdot \frac{1}{4M} = \frac{3}{8b\sqrt{M}} < 1,$$

where the last step stems from the fact that $M, b \geq 1$.

□

Regret Analysis

Theorem 31 (Restatement of Theorem 10). *Suppose Assumptions 2, 3, and 4 hold. There is an absolute value C such that after $\tilde{O}(T_0)$ iterations in Step 1 of Algorithm 1 where T_0 satisfies*

$$T_0^2 \geq Cd_{\mathbf{w}} \iota \max \left\{ \frac{\mu^{\gamma/(2-\gamma)}}{\tau^{2/(2-\gamma)}}, \frac{2C_g^2}{\mu c^2} \right\}$$

with ι denoting a logarithmic term depending on $T_0, C_h, 1/\delta$. Then Algorithm 1 with parameters $T_0 = \sqrt{T}, \lambda = T$ satisfies that with probability at least $1 - \delta$,

$$R_T = O\left(d_w^2 \log^{\frac{3}{2}}(T) \log(d_w \log(T))\right).$$

Proof. Since Algorithm 1 runs in multiple stages where the same action is played for multiple rounds, so we first focus on the instantaneous regret of one round in each stage and then calculate the cumulative regret in all stages. At stage s , the instantaneous regret of one round r_s is defined as

$$r_s = f_0(\mathbf{x}^*) - f_0(\mathbf{x}_s) = f_{\mathbf{x}^*}(\mathbf{w}^*) - f_{\mathbf{x}_s}(\mathbf{w}^*),$$

where the second equation is due to Assumption 2. Recall that the selection process of \mathbf{x}_s in Algorithm 1 is

$$\mathbf{x}_s = \arg \max_{\mathbf{x} \in \mathcal{X}} \max_{\mathbf{w} \in \text{Ball}_s} f_{\mathbf{x}}(\mathbf{w}),$$

and we define $\tilde{\mathbf{w}}$ to be the parameter that maximizes the function value at \mathbf{x}_s , i.e., $\tilde{\mathbf{w}} = \arg \max_{\mathbf{w} \in \text{Ball}_s} f_{\mathbf{x}_s}(\mathbf{w})$, then we have

$$r_s \leq f_{\mathbf{x}_s}(\tilde{\mathbf{w}}) - f_{\mathbf{x}_s}(\mathbf{w}^*) = (\tilde{\mathbf{w}} - \mathbf{w}^*)^\top \nabla f_{\mathbf{x}_s}(\hat{\mathbf{w}}),$$

where the equation is by first order Taylor's theorem and $\hat{\mathbf{w}}$ is a parameter lying between $\tilde{\mathbf{w}}$ and \mathbf{w}^* . Due to the convex structure of Ball_s for each stage s , it implies that $\hat{\mathbf{w}} \in \text{Ball}_s$. By adding and removing $\hat{\mathbf{w}}_s$ and $\nabla f_{\mathbf{x}_s}(\hat{\mathbf{w}}_0)$, we have

$$\begin{aligned}
r_s &\leq (\tilde{\mathbf{w}} - \hat{\mathbf{w}}_s + \hat{\mathbf{w}}_s - \mathbf{w}^*)^\top (\nabla f_{\mathbf{x}_s}(\hat{\mathbf{w}}_0) - \nabla f_{\mathbf{x}_s}(\hat{\mathbf{w}}_0) + \nabla f_{\mathbf{x}_s}(\hat{\mathbf{w}})), \\
&= (\tilde{\mathbf{w}} - \hat{\mathbf{w}}_s)^\top \nabla f_{\mathbf{x}_s}(\hat{\mathbf{w}}_0) + (\hat{\mathbf{w}}_s - \mathbf{w}^*)^\top \nabla f_{\mathbf{x}_s}(\hat{\mathbf{w}}_0)
\end{aligned}$$

$$\begin{aligned}
& + (\tilde{\mathbf{w}} - \hat{\mathbf{w}}_s + \hat{\mathbf{w}}_s - \mathbf{w}^*)^\top (\nabla f_{\mathbf{x}_s}(\dot{\mathbf{w}}_s) - \nabla f_{\mathbf{x}_s}(\hat{\mathbf{w}}_0)), \\
\leq & \|\tilde{\mathbf{w}} - \hat{\mathbf{w}}_s\|_{\Sigma_s} \|\nabla f_{\mathbf{x}_s}(\hat{\mathbf{w}}_0)\|_{\Sigma_s^{-1}} + \|\hat{\mathbf{w}}_s - \mathbf{w}^*\|_{\Sigma_s} \|\nabla f_{\mathbf{x}_s}(\hat{\mathbf{w}}_0)\|_{\Sigma_s^{-1}} \\
& + (\tilde{\mathbf{w}} - \hat{\mathbf{w}}_s + \hat{\mathbf{w}}_s - \mathbf{w}^*)^\top (\nabla f_{\mathbf{x}_s}(\dot{\mathbf{w}}_s) - \nabla f_{\mathbf{x}_s}(\hat{\mathbf{w}}_0)),
\end{aligned}$$

where the last inequality is due to Holder's inequality.

Since both $\tilde{\mathbf{w}}$ and \mathbf{w}^* are in Ball_s and $\epsilon_s = \|\nabla f_{\mathbf{x}_s}(\hat{\mathbf{w}}_0)\|_{\Sigma_s^{-1}}$, we have

$$r_s \leq 2\sqrt{\beta_s}\epsilon_s + (\tilde{\mathbf{w}} - \hat{\mathbf{w}}_s + \hat{\mathbf{w}}_s - \mathbf{w}^*)^\top (\nabla f_{\mathbf{x}_s}(\dot{\mathbf{w}}) - \nabla f_{\mathbf{x}_s}(\hat{\mathbf{w}}_0)).$$

Again by first order Taylor's theorem where $\ddot{\mathbf{w}}$ lies between $\dot{\mathbf{w}}$ and $\hat{\mathbf{w}}_0$, we have

$$\begin{aligned}
r_s & \leq 2\sqrt{\beta_s}\epsilon_s + (\tilde{\mathbf{w}} - \hat{\mathbf{w}}_s + \hat{\mathbf{w}}_s - \mathbf{w}^*)^\top \nabla^2 f_{\mathbf{x}_s}(\ddot{\mathbf{w}})(\dot{\mathbf{w}} - \hat{\mathbf{w}}_0), \\
& = 2\sqrt{\beta_s}\epsilon_s + (\tilde{\mathbf{w}} - \hat{\mathbf{w}}_s + \hat{\mathbf{w}}_s - \mathbf{w}^*)^\top \nabla^2 f_{\mathbf{x}_s}(\ddot{\mathbf{w}})(\dot{\mathbf{w}} - \hat{\mathbf{w}}_s + \hat{\mathbf{w}}_s - \mathbf{w}^* + \mathbf{w}^* - \hat{\mathbf{w}}_0), \\
& = 2\sqrt{\beta_s}\epsilon_s + (\tilde{\mathbf{w}} - \hat{\mathbf{w}}_s + \hat{\mathbf{w}}_s - \mathbf{w}^*)^\top \Sigma_s^{\frac{1}{2}} \Sigma_s^{-\frac{1}{2}} \nabla^2 f_{\mathbf{x}_s}(\ddot{\mathbf{w}}) \Sigma_s^{\frac{1}{2}} \Sigma_s^{-\frac{1}{2}} (\dot{\mathbf{w}} - \hat{\mathbf{w}}_s + \hat{\mathbf{w}}_s - \mathbf{w}^* + \mathbf{w}^* - \hat{\mathbf{w}}_0), \\
& = 2\sqrt{\beta_s}\epsilon_s + (\tilde{\mathbf{w}} - \hat{\mathbf{w}}_s)^\top \Sigma_s^{\frac{1}{2}} \Sigma_s^{-\frac{1}{2}} \nabla^2 f_{\mathbf{x}_s}(\ddot{\mathbf{w}}) \Sigma_s^{-\frac{1}{2}} \Sigma_s^{\frac{1}{2}} (\hat{\mathbf{w}}_s - \hat{\mathbf{w}}_s) \\
& \quad + (\tilde{\mathbf{w}} - \hat{\mathbf{w}}_s)^\top \Sigma_s^{\frac{1}{2}} \Sigma_s^{-\frac{1}{2}} \nabla^2 f_{\mathbf{x}_s}(\ddot{\mathbf{w}}) \Sigma_s^{-\frac{1}{2}} \Sigma_s^{\frac{1}{2}} (\hat{\mathbf{w}}_s - \mathbf{w}^*) \\
& \quad + (\tilde{\mathbf{w}} - \hat{\mathbf{w}}_s)^\top \Sigma_s^{\frac{1}{2}} \Sigma_s^{-\frac{1}{2}} \nabla^2 f_{\mathbf{x}_s}(\ddot{\mathbf{w}}) \Sigma_s^{-\frac{1}{2}} \Sigma_s^{\frac{1}{2}} (\mathbf{w}^* - \hat{\mathbf{w}}_0) \\
& \quad + (\hat{\mathbf{w}}_s - \mathbf{w}^*)^\top \Sigma_s^{\frac{1}{2}} \Sigma_s^{-\frac{1}{2}} \nabla^2 f_{\mathbf{x}_s}(\ddot{\mathbf{w}}) \Sigma_s^{-\frac{1}{2}} \Sigma_s^{\frac{1}{2}} (\dot{\mathbf{w}} - \hat{\mathbf{w}}_s) \\
& \quad + (\hat{\mathbf{w}}_s - \mathbf{w}^*)^\top \Sigma_s^{\frac{1}{2}} \Sigma_s^{-\frac{1}{2}} \nabla^2 f_{\mathbf{x}_s}(\ddot{\mathbf{w}}) \Sigma_s^{-\frac{1}{2}} \Sigma_s^{\frac{1}{2}} (\hat{\mathbf{w}}_s - \mathbf{w}^*) \\
& \quad + (\hat{\mathbf{w}}_s - \mathbf{w}^*)^\top \Sigma_s^{\frac{1}{2}} \Sigma_s^{-\frac{1}{2}} \nabla^2 f_{\mathbf{x}_s}(\ddot{\mathbf{w}}) \Sigma_s^{-\frac{1}{2}} \Sigma_s^{\frac{1}{2}} (\mathbf{w}^* - \hat{\mathbf{w}}_0), \\
& \leq 2\sqrt{\beta_s}\epsilon_s + \|(\tilde{\mathbf{w}} - \hat{\mathbf{w}}_s)^\top \Sigma_s^{\frac{1}{2}}\|_2 \|\Sigma_s^{-\frac{1}{2}} \nabla^2 f_{\mathbf{x}_s}(\ddot{\mathbf{w}}) \Sigma_s^{-\frac{1}{2}}\|_{\text{op}} \|\Sigma_s^{\frac{1}{2}} (\dot{\mathbf{w}} - \hat{\mathbf{w}}_s)\|_2 \\
& \quad + \|(\tilde{\mathbf{w}} - \hat{\mathbf{w}}_s)^\top \Sigma_s^{\frac{1}{2}}\|_2 \|\Sigma_s^{-\frac{1}{2}} \nabla^2 f_{\mathbf{x}_s}(\ddot{\mathbf{w}}) \Sigma_s^{-\frac{1}{2}}\|_{\text{op}} \|\Sigma_s^{\frac{1}{2}} (\hat{\mathbf{w}}_s - \mathbf{w}^*)\|_2 \\
& \quad + \|(\tilde{\mathbf{w}} - \hat{\mathbf{w}}_s)^\top \Sigma_s^{\frac{1}{2}}\|_2 \|\Sigma_s^{-\frac{1}{2}} \nabla^2 f_{\mathbf{x}_s}(\ddot{\mathbf{w}}) \Sigma_s^{-\frac{1}{2}}\|_{\text{op}} \|\Sigma_s^{\frac{1}{2}} (\mathbf{w}^* - \hat{\mathbf{w}}_0)\|_2 \\
& \quad + \|(\hat{\mathbf{w}}_s - \mathbf{w}^*)^\top \Sigma_s^{\frac{1}{2}}\|_2 \|\Sigma_s^{-\frac{1}{2}} \nabla^2 f_{\mathbf{x}_s}(\ddot{\mathbf{w}}) \Sigma_s^{-\frac{1}{2}}\|_{\text{op}} \|\Sigma_s^{\frac{1}{2}} (\dot{\mathbf{w}} - \hat{\mathbf{w}}_s)\|_2 \\
& \quad + \|(\hat{\mathbf{w}}_s - \mathbf{w}^*)^\top \Sigma_s^{\frac{1}{2}}\|_2 \|\Sigma_s^{-\frac{1}{2}} \nabla^2 f_{\mathbf{x}_s}(\ddot{\mathbf{w}}) \Sigma_s^{-\frac{1}{2}}\|_{\text{op}} \|\Sigma_s^{\frac{1}{2}} (\hat{\mathbf{w}}_s - \mathbf{w}^*)\|_2 \\
& \quad + \|(\hat{\mathbf{w}}_s - \mathbf{w}^*)^\top \Sigma_s^{\frac{1}{2}}\|_2 \|\Sigma_s^{-\frac{1}{2}} \nabla^2 f_{\mathbf{x}_s}(\ddot{\mathbf{w}}) \Sigma_s^{-\frac{1}{2}}\|_{\text{op}} \|\Sigma_s^{\frac{1}{2}} (\mathbf{w}^* - \hat{\mathbf{w}}_0)\|_2,
\end{aligned}$$

where the second line is by adding and removing $\hat{\mathbf{w}}_s$ and \mathbf{w}^* and the last inequality is due to Holder's inequality. Since the center of Ball_s is $\hat{\mathbf{w}}_s$ and \mathbf{w}^* , $\tilde{\mathbf{w}}, \dot{\mathbf{w}} \in \text{Ball}_s$, then we have

$$\begin{aligned}
r_s & \leq 2\sqrt{\beta_s}\epsilon_s + 4\beta_s \|\Sigma_s^{-\frac{1}{2}} \nabla^2 f_{\mathbf{x}_s}(\ddot{\mathbf{w}}) \Sigma_s^{-\frac{1}{2}}\|_{\text{op}} + 2\sqrt{\beta_s} \|\Sigma_s^{-\frac{1}{2}} \nabla^2 f_{\mathbf{x}_s}(\ddot{\mathbf{w}}) \Sigma_s^{-\frac{1}{2}}\|_{\text{op}} \|\Sigma_s^{\frac{1}{2}} (\mathbf{w}^* - \hat{\mathbf{w}}_0)\|_2, \\
& \leq 2\sqrt{\beta_s}\epsilon_s + 4\beta_s \|\Sigma_s^{-\frac{1}{2}} \nabla^2 f_{\mathbf{x}_s}(\ddot{\mathbf{w}}) \Sigma_s^{-\frac{1}{2}}\|_{\text{op}} + 2\sqrt{\beta_s} \|\Sigma_s^{-\frac{1}{2}} \nabla^2 f_{\mathbf{x}_s}(\ddot{\mathbf{w}}) \Sigma_s^{-\frac{1}{2}}\|_{\text{op}} \|\Sigma_s^{\frac{1}{2}}\|_{\text{op}} \|\mathbf{w}^* - \hat{\mathbf{w}}_0\|_2, \\
& \leq 2\sqrt{\beta_s}\epsilon_s + \frac{4\beta_s C_h}{\lambda} + \frac{2\sqrt{\beta_s} C_h C_0}{T_0 \sqrt{\lambda}},
\end{aligned}$$

where the second inequality is again due to Holder's inequality and the last inequality is by Assumption 3, the choice of Σ_s , and convergence guarantee of $\hat{\mathbf{w}}_0$.

Recall that in stage s , the algorithm plays actions x_s for $\frac{C_1}{\epsilon_s} \log \frac{m}{\delta}$ rounds, therefore, the cumulative regret in stage s is bounded as

$$\frac{C_1}{\epsilon_s} \left(2\sqrt{\beta_s}\epsilon_s + \frac{4\beta_s C_h}{\lambda} + \frac{2\sqrt{\beta_s} C_h C_0}{T_0 \sqrt{\lambda}} \right) \log \left(\frac{m}{\delta} \right).$$

In total, there are m stages, so the cumulative regret is bounded as

$$\begin{aligned}
R_T & \leq \sum_{s=1}^m \frac{C_1}{\epsilon_s} \left(2\sqrt{\beta_s}\epsilon_s + \frac{4\beta_s C_h}{\lambda} + \frac{2\sqrt{\beta_s} C_h C_0}{T_0 \sqrt{\lambda}} \right) \log \left(\frac{m}{\delta} \right), \\
& = 2C_1 \log \left(\frac{m}{\delta} \right) \sum_{s=1}^m \left(\sqrt{\beta_s} + \frac{2\beta_s C_h}{\epsilon_s \lambda} + \frac{\sqrt{\beta_s} C_h C_0}{\epsilon_s T_0 \sqrt{\lambda}} \right).
\end{aligned}$$

Recall that our choice of β_s is

$$\beta_s = 3d_w s + \frac{3\lambda C_0^2}{T_0^2} + \frac{3C_h^2 C_0^2 s T^2}{4T_0^4},$$

which is increasing in s , so $\beta_s \leq \beta_m$ where m is the number of stages. Therefore, we have

$$\begin{aligned} R_T &\leq 2C_1 \log\left(\frac{m}{\delta}\right) \left(m\sqrt{\beta_m} + \left(\frac{2\beta_m C_h}{\lambda} + \frac{\sqrt{\beta_m} C_h C_0}{T_0 \sqrt{\lambda}} \right) \sum_{s=1}^m \frac{1}{\epsilon_s} \right), \\ &\leq 2C_1 \log\left(\frac{m}{\delta}\right) \left(m\sqrt{\beta_m} + \frac{2\beta_m C_h T}{\lambda} + \frac{\sqrt{\beta_m} C_h C_0 T}{T_0 \sqrt{\lambda}} \right), \end{aligned}$$

where the second inequality is due to Lemma 16.

Now plug in our choices $T_0 = \sqrt{T}$, $\lambda = T$ (they are reverse-engineered to make the analysis work) and maximum stage number $m = d_w \log\left(\frac{C_g^2 T}{d_w} + 1\right)$ (Lemma 13), and we have

$$\begin{aligned} R_T &\leq 2C_1 \log\left(\frac{m}{\delta}\right) \left(m\sqrt{\beta_m} + 2\beta_m C_h + \sqrt{\beta_m} C_h C_0 \right), \\ \beta_m &= 3d_w m + 3C_0^2 + \frac{3C_h^2 C_0^2 m}{4} = O(d_w m). \end{aligned}$$

Reorganize them and we have

$$\begin{aligned} R_T &= O\left((m\sqrt{d_w m} + d_w m) \log\left(\frac{m}{\delta}\right) \right), \\ &= O\left((d_w \log(T))^{\frac{3}{2}} \sqrt{d_w} + d_w^2 \log(T) \log(d_w \log(T)) \right), \\ &= O\left(d_w^2 \log^{\frac{3}{2}}(T) \log(d_w \log(T)) \right), \end{aligned}$$

which completes the proof. \square

Lemma 32 (Restatement of Lemma 13). *The Algorithm 1 runs at most $m = d_w \log\left(\frac{C_g^2 T^2}{d_w \lambda} + 1\right)$ stages.*

Proof. The proof follows the outline of that for Lemma 2 in (Wan et al. 2023). First, we show that $\det(\Sigma_s) = 2 \det(\Sigma_{s-1})$, $\forall s = 1, 2, \dots, m$.

$$\begin{aligned} \det(\Sigma_s) &= \det\left(\Sigma_{s-1} + \frac{1}{\epsilon_s^2} \nabla f_{\mathbf{x}_s}(\hat{\mathbf{w}}_0) \nabla f_{\mathbf{x}_s}(\hat{\mathbf{w}}_0)^\top \right), \\ &= \det\left(\Sigma_{s-1}^{1/2} \left(\mathbf{I}_{d_w} + \frac{1}{\epsilon_s^2} \Sigma_{s-1}^{-\frac{1}{2}} \nabla f_{\mathbf{x}_s}(\hat{\mathbf{w}}_0) \nabla f_{\mathbf{x}_s}(\hat{\mathbf{w}}_0)^\top \Sigma_{s-1}^{-\frac{1}{2}} \right) \Sigma_{s-1}^{\frac{1}{2}} \right), \\ &= \det(\Sigma_{s-1}) \det\left(\mathbf{I} + \frac{1}{\epsilon_s^2} \Sigma_{s-1}^{-\frac{1}{2}} \nabla f_{\mathbf{x}_s}(\hat{\mathbf{w}}_0) \nabla f_{\mathbf{x}_s}(\hat{\mathbf{w}}_0)^\top \Sigma_{s-1}^{-\frac{1}{2}} \right), \\ &= \det(\Sigma_{s-1}) \left(1 + \frac{1}{\epsilon_s^2} \nabla f_{\mathbf{x}_s}(\hat{\mathbf{w}}_0)^\top \Sigma_{s-1}^{-\frac{1}{2}} \Sigma_{s-1}^{-\frac{1}{2}} \nabla f_{\mathbf{x}_s}(\hat{\mathbf{w}}_0) \right), \\ &= \det(\Sigma_{s-1}) \left(1 + \frac{1}{\epsilon_s^2} \|\nabla f_{\mathbf{x}_s}(\hat{\mathbf{w}}_0)\|_{\Sigma_{s-1}^{-1}}^2 \right), \\ &= 2 \det(\Sigma_{s-1}), \end{aligned}$$

where the fourth line follows from the matrix determinant lemma: $\det(\mathbf{A} + \mathbf{u}\mathbf{v}^\top) = (1 + \mathbf{v}^\top \mathbf{A}^{-1} \mathbf{u}) \det(\mathbf{A})$ where \mathbf{A} is an invertible square matrix and \mathbf{u}, \mathbf{v} are column vectors. Thus, $\det(\Sigma_m) = 2^m \det(\Sigma_0) = 2^m \lambda^{d_w}$.

On the other hand, note that

$$\Sigma_m = \lambda \mathbf{I}_{d_w} + \sum_{s=1}^m \frac{1}{\epsilon_s^2} \nabla f_{\mathbf{x}_s}(\hat{\mathbf{w}}_0) \nabla f_{\mathbf{x}_s}(\hat{\mathbf{w}}_0)^\top,$$

and hence by cyclic property of matrix trace,

$$\text{tr}(\Sigma_m) = d_w \lambda + \sum_{s=1}^m \frac{\|\nabla f_{\mathbf{x}_s}(\hat{\mathbf{w}}_0)\|_2^2}{\epsilon_s^2}.$$

Then by Assumption 3 and the trace-determinant inequality: $d_w \cdot \det(\mathbf{A})^{\frac{1}{d_w}} \leq \text{tr}(\mathbf{A})$, we have

$$d_w \cdot \lambda 2^{\frac{m}{d_w}} \leq d_w \lambda + \sum_{s=1}^m \frac{\|\nabla f_{\mathbf{x}_s}(\hat{\mathbf{w}}_0)\|_2^2}{\epsilon_s^2} \leq d_w \lambda + \sum_{s=1}^m \frac{C_g^2}{\epsilon_s^2},$$

and hence

$$\sum_{s=1}^m \frac{1}{\epsilon_s^2} \geq \frac{d_w \lambda}{C_g^2} (2^{\frac{m}{d_w}} - 1).$$

Note that during each stage s , we query the quantum oracle for $\frac{C_1}{\epsilon_s} \log \frac{m}{\delta}$ times. Then with $C_1 > 1$ and $\delta \in (0, 1/2]$, we have

$$\sum_{s=1}^m \frac{C_1}{\epsilon_s} \log \frac{m}{\delta} \geq \sum_{s=1}^m \frac{1}{\epsilon_s} \geq \sqrt{\sum_{s=1}^m \frac{1}{\epsilon_s^2}} \geq \frac{1}{C_g} \sqrt{d_w \lambda (2^{\frac{m}{d_w}} - 1)}. \quad (9)$$

Now we derive an upper bound on m by contradiction. Suppose $m > d_w \log \left(\frac{C_g^2 T^2}{d_w \lambda} + 1 \right)$. This implies that

$$\sum_{s=1}^m \frac{C_1}{\epsilon_s} \log \frac{m}{\delta} \geq \frac{1}{C_g} \sqrt{d_w \lambda (2^{\frac{m}{d_w}} - 1)} > T,$$

which is a contradiction. Therefore, Q-NLB-UCB algorithm has at most $d_w \log \left(\frac{C_g^2 T^2}{d_w \lambda} + 1 \right)$ stages. \square

Confidence Analysis

Proof Sketch. The proof has two steps. In the first step, we solve the regression problem defined in Eq. (4) to get a closed form solution of $\hat{\mathbf{w}}_s$. Then in the second step, we upper bound multiple terms in $\|\hat{\mathbf{w}}_s - \mathbf{w}^*\|_{\Sigma_s}^2$ and the final upper bound is chosen as the valid β_s .

Lemma 33 (Restatement of Lemma 14). *Suppose Assumptions 2, 3, and 4 hold and β_s is chosen as Eq. (6). Then with parameters $T_0 = \sqrt{T}$, $\lambda = T$ in each stage s in Algorithm 1, the optimal parameter \mathbf{w}^* is trapped in confidence ball Ball_s with probability at least $1 - \delta$, i.e.,*

$$\|\hat{\mathbf{w}}_s - \mathbf{w}^*\|_{\Sigma_s}^2 \leq \beta_s.$$

Proof. By setting the derivative of objective function in Eq. (4) w.r.t. \mathbf{w} as 0, we find the optimal criterion is

$$0 = \lambda(\hat{\mathbf{w}}_s - \hat{\mathbf{w}}_0) + \sum_{i=0}^{s-1} \frac{1}{\epsilon_i^2} ((\hat{\mathbf{w}}_s - \hat{\mathbf{w}}_0)^\top \nabla f_{\mathbf{x}_i}(\hat{\mathbf{w}}_0) + f_{\mathbf{x}_i}(\hat{\mathbf{w}}_0) - y_i) \nabla f_{\mathbf{x}_i}(\hat{\mathbf{w}}_0).$$

Rearrange the equation and we have

$$\begin{aligned} \lambda(\hat{\mathbf{w}}_s - \hat{\mathbf{w}}_0) + \sum_{i=0}^{s-1} \frac{1}{\epsilon_i^2} (\hat{\mathbf{w}}_s - \hat{\mathbf{w}}_0)^\top \nabla f_{\mathbf{x}_i}(\hat{\mathbf{w}}_0) \nabla f_{\mathbf{x}_i}(\hat{\mathbf{w}}_0) &= \sum_{i=0}^{s-1} \frac{1}{\epsilon_i^2} (y_i - f_{\mathbf{x}_i}(\hat{\mathbf{w}}_0)) \nabla f_{\mathbf{x}_i}(\hat{\mathbf{w}}_0), \\ \lambda(\hat{\mathbf{w}}_s - \hat{\mathbf{w}}_0) + \sum_{i=0}^{s-1} \frac{1}{\epsilon_i^2} \hat{\mathbf{w}}_s^\top \nabla f_{\mathbf{x}_i}(\hat{\mathbf{w}}_0) \nabla f_{\mathbf{x}_i}(\hat{\mathbf{w}}_0) &= \sum_{i=0}^{s-1} \frac{1}{\epsilon_i^2} (\hat{\mathbf{w}}_0^\top \nabla f_{\mathbf{x}_i}(\hat{\mathbf{w}}_0) + y_i - f_{\mathbf{x}_i}(\hat{\mathbf{w}}_0)) \nabla f_{\mathbf{x}_i}(\hat{\mathbf{w}}_0), \\ \left(\lambda \mathbf{I} + \sum_{i=0}^{s-1} \frac{1}{\epsilon_i^2} \nabla f_{\mathbf{x}_i}(\hat{\mathbf{w}}_0) \nabla f_{\mathbf{x}_i}(\hat{\mathbf{w}}_0)^\top \right) \hat{\mathbf{w}}_s - \lambda \hat{\mathbf{w}}_0 &= \sum_{i=0}^{s-1} \frac{1}{\epsilon_i^2} (\hat{\mathbf{w}}_0^\top \nabla f_{\mathbf{x}_i}(\hat{\mathbf{w}}_0) + y_i - f_{\mathbf{x}_i}(\hat{\mathbf{w}}_0)) \nabla f_{\mathbf{x}_i}(\hat{\mathbf{w}}_0), \end{aligned}$$

where the third line is due to definition of observation noise ϵ_i . By our choice of Σ_s (Eq. (3)) which is inevitable, we have

$$\Sigma_s \hat{\mathbf{w}}_s = \lambda \hat{\mathbf{w}}_0 + \sum_{i=0}^{s-1} \frac{1}{\epsilon_i^2} (\hat{\mathbf{w}}_0^\top \nabla f_{\mathbf{x}_i}(\hat{\mathbf{w}}_0) + y_i - f_{\mathbf{x}_i}(\hat{\mathbf{w}}_0)) \nabla f_{\mathbf{x}_i}(\hat{\mathbf{w}}_0),$$

And the closed form solution of $\hat{\mathbf{w}}_s$ is shown as:

$$\hat{\mathbf{w}}_s = \Sigma_s^{-1} \left(\lambda \hat{\mathbf{w}}_0 + \sum_{i=0}^{s-1} \frac{1}{\epsilon_i^2} (\hat{\mathbf{w}}_0^\top \nabla f_{\mathbf{x}_i}(\hat{\mathbf{w}}_0) + y_i - f_{\mathbf{x}_i}(\hat{\mathbf{w}}_0)) \nabla f_{\mathbf{x}_i}(\hat{\mathbf{w}}_0) \right).$$

Further, $\hat{\mathbf{w}}_s - \mathbf{w}^*$ can be written as

$$\begin{aligned}
\hat{\mathbf{w}}_s - \mathbf{w}^* &= \Sigma_s^{-1} \left(\sum_{i=0}^{s-1} \frac{1}{\epsilon_i^2} \nabla f_{\mathbf{x}_i}(\hat{\mathbf{w}}_0) (\nabla f_{\mathbf{x}_i}(\hat{\mathbf{w}}_0)^\top \hat{\mathbf{w}}_0 + y_i - f_{\mathbf{x}_i}(\hat{\mathbf{w}}_0)) \right) + \lambda \Sigma_s^{-1} \hat{\mathbf{w}}_0 - \Sigma_s^{-1} \Sigma_s \mathbf{w}^*, \\
&= \Sigma_s^{-1} \left(\sum_{i=0}^{s-1} \frac{1}{\epsilon_i^2} \nabla f_{\mathbf{x}_i}(\hat{\mathbf{w}}_0) (\nabla f_{\mathbf{x}_i}(\hat{\mathbf{w}}_0)^\top \hat{\mathbf{w}}_0 + y_i - f_{\mathbf{x}_i}(\hat{\mathbf{w}}_0)) \right) + \lambda \Sigma_s^{-1} (\hat{\mathbf{w}}_0 - \mathbf{w}^*) \\
&\quad - \Sigma_s^{-1} \left(\sum_{i=0}^{s-1} \frac{1}{\epsilon_i^2} \nabla f_{\mathbf{x}_i}(\hat{\mathbf{w}}_0) \nabla f_{\mathbf{x}_i}(\hat{\mathbf{w}}_0)^\top \right) \mathbf{w}^*, \\
&= \Sigma_s^{-1} \left(\sum_{i=0}^{s-1} \frac{1}{\epsilon_i^2} \nabla f_{\mathbf{x}_0}(\hat{\mathbf{w}}_0) (\nabla f_{\mathbf{x}_i}(\hat{\mathbf{w}}_0)^\top (\hat{\mathbf{w}}_0 - \mathbf{w}^*) + f_{\mathbf{x}_i}(\mathbf{w}^*) - f_{\mathbf{x}_i}(\hat{\mathbf{w}}_0)) + y_i - f_{\mathbf{x}_i}(\hat{\mathbf{w}}_0) \right) \\
&\quad + \lambda \Sigma_s^{-1} (\hat{\mathbf{w}}_0 - \mathbf{w}^*), \\
&= \Sigma_s^{-1} \left(\sum_{i=0}^{s-1} \frac{1}{\epsilon_i^2} \nabla f_{\mathbf{x}_i}(\hat{\mathbf{w}}_0) (\nabla f_{\mathbf{x}_i}(\hat{\mathbf{w}}_0)^\top (\hat{\mathbf{w}}_0 - \mathbf{w}^*) + f_{\mathbf{x}_i}(\mathbf{w}^*) - f_{\mathbf{x}_i}(\hat{\mathbf{w}}_0)) \right) \\
&\quad + \Sigma_s^{-1} \left(\sum_{i=0}^{s-1} \frac{1}{\epsilon_i^2} \nabla f_{\mathbf{x}_i}(\hat{\mathbf{w}}_0) (y_i - f_{\mathbf{x}_i}(\mathbf{w}^*)) \right) + \lambda \Sigma_s^{-1} (\hat{\mathbf{w}}_0 - \mathbf{w}^*), \\
&= \Sigma_s^{-1} \left(\sum_{i=0}^{s-1} \frac{1}{\epsilon_i^2} \nabla f_{\mathbf{x}_i}(\hat{\mathbf{w}}_0) \frac{1}{2} \|\mathbf{w}^* - \hat{\mathbf{w}}_0\|_{\nabla^2 f_{\mathbf{x}_i}(\tilde{\mathbf{w}})}^2 \right) \\
&\quad + \Sigma_s^{-1} \left(\sum_{i=0}^{s-1} \frac{1}{\epsilon_i^2} \nabla f_{\mathbf{x}_i}(\hat{\mathbf{w}}_0) (y_i - f_{\mathbf{x}_i}(\mathbf{w}^*)) \right) + \lambda \Sigma_s^{-1} (\hat{\mathbf{w}}_0 - \mathbf{w}^*), \tag{10}
\end{aligned}$$

where the second line is again by our choice of Σ_s and the last equation is by the second order Taylor's theorem of $f_{\mathbf{x}_i}(\mathbf{w}^*)$ at $\hat{\mathbf{w}}_0$ where $\tilde{\mathbf{w}}$ lies between \mathbf{w}^* and $\hat{\mathbf{w}}_0$.

Multiply both sides of Eq. (10) by $\Sigma_s^{\frac{1}{2}}$ and we have

$$\begin{aligned}
\Sigma_s^{\frac{1}{2}} (\hat{\mathbf{w}}_s - \mathbf{w}^*) &= \frac{1}{2} \Sigma_s^{-\frac{1}{2}} \left(\sum_{i=0}^{s-1} \frac{1}{\epsilon_i^2} \nabla f_{\mathbf{x}_i}(\hat{\mathbf{w}}_0) \|\mathbf{w}^* - \hat{\mathbf{w}}_0\|_{\nabla^2 f_{\mathbf{x}_i}(\tilde{\mathbf{w}})}^2 \right) \\
&\quad + \Sigma_s^{-\frac{1}{2}} \left(\sum_{i=0}^{s-1} \frac{1}{\epsilon_i^2} \nabla f_{\mathbf{x}_i}(\hat{\mathbf{w}}_0) (y_i - f_{\mathbf{x}_i}(\mathbf{w}^*)) \right) + \lambda \Sigma_s^{-\frac{1}{2}} (\hat{\mathbf{w}}_0 - \mathbf{w}^*).
\end{aligned}$$

Take square of both sides and by inequality $(a + b + c)^2 \leq 3(a^2 + b^2 + c^2)$ and we obtain

$$\begin{aligned}
\|\hat{\mathbf{w}}_s - \mathbf{w}^*\|_{\Sigma_s}^2 &\leq 3 \underbrace{\left\| \sum_{i=0}^{s-1} \frac{1}{\epsilon_i^2} \nabla f_{\mathbf{x}_i}(\hat{\mathbf{w}}_0) (y_i - f_{\mathbf{x}_i}(\mathbf{w}^*)) \right\|_{\Sigma_s^{-1}}^2}_{(a)} + \underbrace{3\lambda^2 \|\hat{\mathbf{w}}_0 - \mathbf{w}^*\|_{\Sigma_s^{-1}}^2}_{(b)} \\
&\quad + \frac{3}{4} \underbrace{\left\| \sum_{i=0}^{s-1} \frac{1}{\epsilon_i^2} \nabla f_{\mathbf{x}_i}(\hat{\mathbf{w}}_0) \|\mathbf{w}^* - \hat{\mathbf{w}}_0\|_{\nabla^2 f_{\mathbf{x}_i}(\tilde{\mathbf{w}})}^2 \right\|_{\Sigma_s^{-1}}^2}_{(c)}. \tag{11}
\end{aligned}$$

Now we bound terms (a), (b), (c) separately.

Bounding (a). Let

$$\begin{aligned}
\mathbf{E}_s &= \text{diag}(1/\epsilon_0^2, \dots, 1/\epsilon_{s-1}^2), \\
\mathbf{G}_s &= [\nabla f_{\mathbf{x}_0}(\hat{\mathbf{w}}_0), \dots, \nabla f_{\mathbf{x}_{s-1}}(\hat{\mathbf{w}}_0)]^\top, \\
\mathbf{f}_s &= [f_{\mathbf{x}_0}(\mathbf{w}^*), \dots, f_{\mathbf{x}_{s-1}}(\mathbf{w}^*)], \\
\mathbf{y}_s &= [y_0, \dots, y_{s-1}],
\end{aligned}$$

then (a) can be rewritten as:

$$(a) = 3 \left\| \mathbf{G}_s^\top \mathbf{E}_s (\mathbf{f}_s - \mathbf{y}_s) \right\|_{\Sigma_s^{-1}}^2.$$

Define $\Gamma_s = \mathbf{E}_s^{\frac{1}{2}} (\mathbf{y}_s - \mathbf{f}_s) \in \mathbb{R}^s$. Then

$$\begin{aligned} (a) &= 3 \left\| \mathbf{G}_s^\top \mathbf{E}_s^{\frac{1}{2}} \Gamma_s \right\|_{\Sigma_s^{-1}}^2, \\ &= 3 \Gamma_s^\top \mathbf{E}_s^{\frac{1}{2}} \mathbf{G}_s \Sigma_s^{-1} \mathbf{G}_s^\top \mathbf{E}_s^{\frac{1}{2}} \Gamma_s, \\ &\leq 3 \left\| \Gamma_s \right\|_2^2 \cdot \left\| \mathbf{E}_s^{\frac{1}{2}} \mathbf{G}_x \Sigma_s^{-1} \mathbf{G}_s^\top \mathbf{E}_s^{\frac{1}{2}} \right\|_2, \\ &\leq 3s \cdot \left\| \Gamma_s \right\|_\infty^2 \cdot \text{tr}(\mathbf{E}_s^{\frac{1}{2}} \mathbf{G}_x \Sigma_s^{-1} \mathbf{G}_s^\top \mathbf{E}_s^{\frac{1}{2}}), \\ &\leq 3s \cdot \text{tr}(\Sigma_s^{-1} \mathbf{G}_s^\top \mathbf{E}_s \mathbf{G}_s), \\ &= 3s \cdot \text{tr}(\mathbf{I}_{d_w} - \lambda \Sigma_s^{-1}), \\ &\leq 3d_w s, \end{aligned}$$

where the first inequality is due to Cauchy-Schwarz inequality, the second inequality is by property of ℓ_2 norm, and the third inequality is due to $|f_{\mathbf{x}_i}(\mathbf{w}^*) - y_i| \leq \epsilon_i, \forall i \in [s]$ (Lemma 1), and definition of $\Sigma_s = \lambda \mathbf{I} + \mathbf{G}_s \mathbf{E}_s \mathbf{G}_s^\top$.

Bounding (b). Then (b) can be bounded as:

$$(b) \leq 3\lambda^2 \left\| \Sigma_s^{-1} \right\|_{\text{op}} \left\| \hat{\mathbf{w}} - \mathbf{w}^* \right\|_2^2 \leq 3\lambda \left\| \hat{\mathbf{w}} - \mathbf{w}^* \right\|_2^2 \leq \frac{3\lambda C_0^2}{T_0^2},$$

where the first inequality is by Holder's inequality, the second inequality is due to property of Σ_s and the last inequality follows from Eq. (2).

Bounding (c). Next, (c) can be rewritten and bounded as

$$\begin{aligned} (c) &\leq \frac{3}{4} \left\| \sum_{i=0}^{s-1} \frac{1}{\epsilon_i^2} \nabla f_{\mathbf{x}_i}(\hat{\mathbf{w}}_0) \left\| \nabla^2 f_{\mathbf{x}_i}(\tilde{\mathbf{w}}) \right\|_{\text{op}} \left\| \mathbf{w}^* - \hat{\mathbf{w}}_0 \right\|_2 \right\|_{\Sigma_s^{-1}}^2, \\ &\leq \frac{3}{4} \left\| \sum_{i=0}^{s-1} \frac{C_h C_0^2}{\epsilon_i^2 T_0^2} \nabla f_{\mathbf{x}_i}(\hat{\mathbf{w}}_0) \right\|_{\Sigma_s^{-1}}^2, \\ &= \frac{3C_h^2 C_0^2}{4T_0^4} \left\| \sum_{i=0}^{s-1} \frac{1}{\epsilon_i^2} \nabla f_{\mathbf{x}_i}(\hat{\mathbf{w}}_0) \right\|_{\Sigma_s^{-1}}^2, \end{aligned} \tag{12}$$

where the first inequality is due to Holder's inequality, the second inequality is due to Assumption 3 and Eq. (2). Further we can rewrite Eq. (12) as

$$\begin{aligned} \frac{3C_h^2 C_0^2}{4T_0^4} \left\| \sum_{i=0}^{s-1} \frac{1}{\epsilon_i^2} \nabla f_{\mathbf{x}_i}(\hat{\mathbf{w}}_0) \right\|_{\Sigma_s^{-1}}^2 &= \frac{3C_h^2 C_0^2}{4T_0^4} \left(\sum_{i=0}^{s-1} \frac{1}{\epsilon_i^2} \nabla f_{\mathbf{x}_i}(\hat{\mathbf{w}}_0) \right)^\top \Sigma_s^{-1} \left(\sum_{j=0}^{s-1} \frac{1}{\epsilon_j^2} \nabla f_{\mathbf{x}_j}(\hat{\mathbf{w}}_0) \right), \\ &= \frac{3C_h^2 C_0^2}{4T_0^4} \sum_{i=0}^{s-1} \sum_{j=0}^{s-1} \frac{1}{\epsilon_i^2 \epsilon_j^2} \nabla f_{\mathbf{x}_i}(\hat{\mathbf{w}}_0)^\top \Sigma_s^{-1} \nabla f_{\mathbf{x}_j}(\hat{\mathbf{w}}_0), \\ &\leq \frac{3C_h^2 C_0^2}{4T_0^4} \sum_{i=0}^{s-1} \sum_{j=0}^{s-1} \frac{1}{\epsilon_i^2 \epsilon_j^2} \left\| \nabla f_{\mathbf{x}_i}(\hat{\mathbf{w}}_0) \right\|_{\Sigma_s^{-1}} \left\| \nabla f_{\mathbf{x}_j}(\hat{\mathbf{w}}_0) \right\|_{\Sigma_s^{-1}}, \\ &= \frac{3C_h^2 C_0^2}{4T_0^4} \left(\sum_{i=0}^{s-1} \frac{1}{\epsilon_i^2} \left\| \nabla f_{\mathbf{x}_i}(\hat{\mathbf{w}}_0) \right\|_{\Sigma_s^{-1}} \right) \left(\sum_{j=0}^{s-1} \frac{1}{\epsilon_j^2} \left\| \nabla f_{\mathbf{x}_j}(\hat{\mathbf{w}}_0) \right\|_{\Sigma_s^{-1}} \right), \\ &= \frac{3C_h^2 C_0^2}{4T_0^4} \left(\sum_{i=0}^{s-1} \frac{1}{\epsilon_i} \right) \left(\sum_{j=0}^{s-1} \frac{1}{\epsilon_j} \right), \\ &\leq \frac{3C_h^2 C_0^2}{4T_0^4} \left(\sum_{i=0}^{s-1} \frac{1}{\epsilon_i^2} \right) \left(\sum_{i=0}^{s-1} 1 \right), \end{aligned}$$

$$\begin{aligned} &\leq \frac{3C_h^2 C_0^2 s}{4T_0^4} \left(\sum_{i=0}^{s-1} \frac{1}{\epsilon_i^2} \right), \\ &\leq \frac{3C_h^2 C_0^2 s T^2}{4T_0^4}, \end{aligned}$$

where the first and second inequalities are due to Cauchy-Schwarz inequality and the last inequality is by Lemma 16.

Combine (a), (b), and (c), and we have:

$$\|\hat{\mathbf{w}}_s - \mathbf{w}^*\|_{\Sigma_s}^2 \leq 3d_w s + \frac{3\lambda C_0^2}{T_0^2} + \frac{3C_h^2 C_0^2 s T^2}{4T_0^4}, \quad (13)$$

which reflects our choice of β_s . □

Time Complexity Analysis

In this section, we show the time complexity of Q-NLB-UCB compared with other quantum bandit algorithms. The time complexity of Q-NLB-UCB is demonstrated to be lower than that of other quantum non-linear bandit algorithms in terms of T .

Algorithm	Quantum part	Classical part
Q-GP-UCB	$O(TU_0)$	$O(d_x^4 (\log T)^4)$
QMCKernelUCB	$O(TU_0)$	$O(d_x^4 (\log T)^4)$
Q-NLB-UCB (ours)	$O(TU_0)$	$O(d_w^4 \log T)$

Table 2: Time complexity comparison

We show the time complexity of Q-NLB-UCB in Table 2 in comparison with Q-GP-UCB (Dai et al. 2023) and QMCKernelUCB (Hikima et al. 2024). The time complexity is analyzed in their quantum parts and classical parts, respectively. Let U_0 denote the cost for one query of quantum oracle, then all algorithms have quantum time complexity $O(TU_0)$ since they all run in T rounds.

However, in the classical part, we can see that our Q-NLB-UCB algorithm enjoys a better time complexity in terms of T . Note d_w denotes parameter dimension and d_x denotes input dimension. In Algorithm 1, line 3,4,5,6 and 7 are all classical steps, and their time complexity is dominated by inversion of the covariance matrix $\Sigma_s \in \mathbf{R}^{d_w \times d_w}$, which requires time complexity $O(d_w^3)$. Therefore, total classical time complexity of Q-NLB-UCB becomes $O(m d_w^3) = O(d_w^4 \log T)$. While in Q-GP-UCB and QMCKernelUCB, the classical steps are dominated by the kernel matrix inversion, which takes $O(s^3)$, so the time complexity becomes $O(\sum_{s=1}^m s^3) = O(m^4) = O(d_x^4 (\log T)^4)$ in total.

Details of Experiments

Implementation Details

We publicly release our source code on GitHub <https://github.com/ZakSiam/Quantum-Non-Linear-Bandit-Optimization> to maximize the reproducibility of our work. We also provide full implementation details in this supplement.

For Algorithms An artificial noise variance $\sigma^2 = 0.01$ (aligning with our amplitude-estimation setup) was incorporated when interfacing with the quantum subroutine. The regression oracle in Q-NLB-UCB is approximated by the stochastic gradient descent algorithm on our two layer neural network model utilizing the mean squared error loss, 2000 iterations and 10^{-3} learning rate. Cross-optimization problem in Step 6 of Q-NLB-UCB is approximated by the iterative gradient ascent algorithm over \mathbf{x} and \mathbf{w} with 2000 iterations. We set the learning rate of \mathbf{x} and \mathbf{w} to 10^{-3} for the synthetic experiments, and 10^{-4} for all the AutoML experiments. We set $\lambda = T$, $\beta_s = C \log(s + 1.0)$ with $C = 1.0$, $C_g = 18.0$, $C_1 = 1.0$, and the fail probability $\delta = 0.01$.

We compute the runtime of our Q-NLB-UCB algorithm by recording the wall-clock time (using `time.perf_counter` method in Python) that elapses from just before the main procedure begins until immediately after it terminates. Additionally, we compare the runtime of Q-NLB-UCB with the runtime of Q-GP-UCB and QMCKernelUCB. This runtime encompasses all overheads, such as, circuit construction, data management, amplitude estimation calls etc., providing a fair end-to-end measure for each algorithm under identical conditions while performing the comparative analysis of runtime. In order to ensure consistent hardware and software settings, we run each script separately in the same environment. Finally, the total reported runtime for each algorithm is utilized for direct comparisons.

All experiments were executed locally on a MacBook Pro machine which is equipped with an Apple M4 Pro system-on-chip featuring a 12-core CPU, a 16-core integrated GPU, and a 16-core Neural Engine. It has 24 GB of unified memory shared by the CPU / GPU, and a 512 GB SSD for storage. Code was run under macOS 15 with Python 3.10, PyTorch 2.1, and Qiskit 0.42.1; no external accelerators were used.

For Real-World AutoML Tasks In our AutoML experiments, we delineate that the Q-NLB-UCB algorithm works efficiently in real-world tasks. We particularly focus on three different hyperparameter tuning tasks for three classifiers on two different datasets: Pima Indians Diabetes Database and Breast Cancer Wisconsin (Diagnostic) Dataset. We adopt the Diabetes dataset from Kaggle, and the Breast Cancer dataset from `sklearn.datasets.load_breast_cancer`. Below is the information on dataset licenses.

- **Pima Indians Diabetes Database**¹, released under *CC0: Public Domain*.
- **Breast Cancer Wisconsin (Diagnostic) Dataset**, bundled with `scikit-learn 1.4.2`, original UCI source © Wolberg et al., re-licensed under *CC BY-NC-SA 4.0*.

The diabetes dataset features eight numeric predictors (glucose level, body mass index, number of times pregnant, age, blood pressure, insulin, skin thickness, and diabetes pedigree function) and a binary outcome denoting diabetes or not (1 or 0). On the other hand, the Breast Cancer Wisconsin (Diagnostic) Dataset features 30 real-valued predictive features and a binary outcome (benign or malignant). For each dataset and experiment, we employed the 5-fold cross validation technique by dividing each dataset into 5 folds and then every time using 4 folds for training and remaining 1 fold for testing, in order to reduce the effect of randomness.

We tuned the following eight hyperparameters for the Multi-Layer Perceptron (MLP):

- **Activation function:** The activation function used in the hidden layer. Options include "identity", "logistic", "tanh", or "relu".
- **L2 regularization term:** Strength of the L2 regularization, which helps prevent overfitting. It is a float value sampled from $[10^{-6}, 10^{-2}]$.
- **Initial learning rate:** Initial learning rate used for weight updates. Float in the range $[10^{-6}, 10^{-2}]$.
- **Maximum iterations:** The maximum number of training iterations. Integer value between 100 and 300.
- **Shuffle:** Whether to shuffle samples in each iteration. Boolean value (True or False).
- β_1 : Exponential decay rate for estimates of the first moment vector. Float in the open interval (0, 1).
- β_2 : Exponential decay rate for estimates of the second moment vector. Float in the open interval (0, 1).
- **Max epochs without improvement:** The maximum number of epochs to not meet the tolerance improvement. Integer between 1 and 10.

We tuned the following eleven hyperparameters for Gradient Boosting (GB):

- **Loss:** The loss function to be optimized. Options include "log_loss" or "exponential".
- **Learning rate:** A float in the open interval (0, 1) controlling the contribution of each tree.
- **Number of estimators:** The total number of boosting stages. Integer in [20, 200].
- **Subsample fraction:** The fraction of samples to be used for fitting the individual base learners. Float in the open interval (0, 1).
- **Split quality criterion:** The function to measure the quality of a split. Options include "friedman_mse" or "squared_error".
- **Min samples to split internal node:** Minimum number of samples required to split an internal node. Integer in [2, 10].
- **Min samples at leaf node:** Minimum number of samples required to be at a leaf node. Integer in [1, 10].
- **Min weight fraction:** Minimum weighted fraction of the sum total of weights required to be at a leaf node. Float in the interval (0, 0.5].
- **Max depth:** Maximum depth of the individual regression estimators. Integer in [1, 10].
- **Number of features:** Number of features to consider when looking for the best split. Options include "sqrt", or "log2".
- **Max leaf nodes:** Maximum number of leaf nodes in best-first fashion. Integer in [2, 10].

We tuned the following four hyperparameters for support vector machine (SVM):

- **C:** The regularization parameter which controls the trade-off between having a smooth decision boundary (smaller C) versus classifying training points accurately (larger C).
- **gamma (γ):** The kernel coefficient (for rbf kernels), which impacts the extent to which a single training sample affects the decision boundary. A higher gamma value generally tends to create more complex boundaries.
- **tol (tolerance):** The stopping tolerance for the solver, specifically the minimal variation in objective value that the solver keeps iterating upon. Lower values result in a more accurate but sometimes slower convergence.

¹<https://www.kaggle.com/datasets/uciml/pima-indians-diabetes-database>

- **kernel:** The functional form which is utilized to map feature vectors into a higher-dimensional space. Common choices for SVC include `linear`, `rbf`, `poly`, and `sigmoid`, each of which can significantly change both model capacity and performance. We only chose `linear` and `rbf` kernels for our experiments.

We employed scikit-learn’s `svm.SVC`, `neural_network.MLPClassifier`, and `ensemble.GradientBoostingClassifier` to train and evaluate the SVM, MLP, and Gradient-Boosting models, respectively, while systematically varying their key hyperparameters through our continuous search embedding. For each learner—SVM (4D), Multi-Layer Perceptron (8D) and Gradient Boosting (11D)— we optimize over a continuous box $\mathcal{X} = [0, 10]^d$ sampled by a scrambled Sobol sequence. Every evaluation point $x \in \mathcal{X}$ is decoded into concrete scikit-learn hyperparameters by simple affine or logarithmic rescaling for numeric fields and by partitioning the interval for categorical choices (e.g. $x_4 < 5$ selects a `linear` SVM kernel, $x_1 < 2.5$ picks the `identity` activation in MLP, $x_1 < 5$ chooses the “`log_loss`” objective in Gradient Boosting). This continuous embedding allows gradient updates while still covering the usual discrete options. The objective returned to the bandit algorithm is the mean test accuracy across the same five pre-generated stratified folds of the Breast-Cancer dataset; all classifiers use `random.state=0` so that variability arises solely from the Sobol-initialized search trajectory.

The primary objective here is to maximize the validation accuracy in both datasets by choosing the optimal set of hyperparameter values. Therefore, the function mapping from hyperparameters to classification accuracy is the black-box function that we aim to maximize for each classifier on each dataset. Cumulative regret was used to evaluate hyperparameter tuning performances, however, since the best accuracy f^* is unknown ahead of time, therefore, it was set to be the best empirical accuracy of each task.

Additional Experimental Results

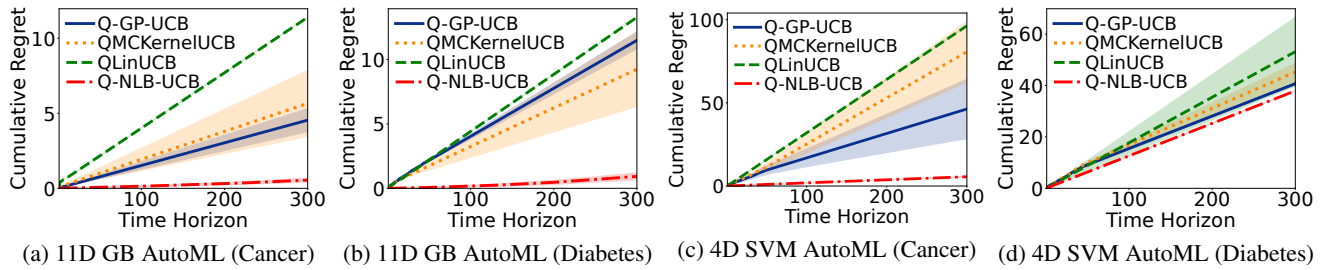


Figure 3: Cumulative regrets (the lower the better) of all compared quantum bandit algorithms.

Stage	Selected action x_s	True reward $f(x_s)$	QME estimated y_s	$ y_s - f(x_s) $
1	$[-0.6, 0.5, -0.1]$	-40.6200	-40.6109	0.0091
2	$[-0.5, 0.4, 0]$	-38.5002	-38.5085	0.0083
3	$[-0.5, 0.3, 0]$	-33.4302	-33.4329	0.0027
4	$[-0.5, 0.3, 0.1]$	-35.3500	-35.3491	0.0009
5	$[-0.5, 0.3, 0.1]$	-35.3500	-35.3486	0.0014

Table 3: Quantum Implementation Results

Stage	Selected action x_s	True reward $f(x_s)$	Classical mean y_s	$ y_s - f(x_s) $
1	$[-0.6, 0.5, -0.1]$	-40.6200	-26.1172	14.5028
2	$[-0.7, 0.5, -0.1]$	-35.7500	-33.2826	2.4674
3	$[-0.6, 0.5, -0.1]$	-40.6200	-40.7809	0.1609
4	$[-0.5, 0.4, 0]$	-38.5002	-36.8721	1.6281
5	$[-0.5, 0.4, 0]$	-38.5002	-40.9617	2.4615

Table 4: Classical Implementation Results

Real-World AutoML Results In the main paper, we only show results on the MLP hyperparameter tuning tasks. Here in Figure 3, we show results on GB and SVM tasks. It again shows that our Q-NLB-UCB algorithm outperforms all the other algorithms by achieving significantly smaller cumulative regret on both datasets.

Our experiments reveal that Q-NLB-UCB can consistently find out the near-optimal Gradient Boosting and SVM hyperparameters while utilizing relatively few queries. The quantum amplitude estimation step in Q-NLB-UCB allows it to refine its hyperparameter selection in a way that balances exploration and exploitation very effectively. The final classification accuracies at the identified hyperparameters were very close to the true maximum of each dataset’s domain, delineating the viability of Q-NLB-UCB as a quantum-inspired powerful tool for hyperparameter tuning on different real-world datasets.

Ablation Experiments on Quality of Quantum Mean Estimator For Step 1 of Q-NLB-UCB in Algorithm 1, while many algorithms have been designed to solve quantum linear regression problems, quantum non-linear regression is still an open problem where no specific algorithm has been developed to achieve the quantum speed-up. Our work in Step 1 proves the existence of a quantum regression oracle that solves this problem, shading the light to develop such a realizable algorithm in the future. Therefore, in experiments, we used classical gradient descent as the surrogate model for Step 1. Even with that, our Q-NLB-UCB algorithm outperforms all other compared quantum bandit algorithms.

For Step 9 in Algorithm 1, we have conducted the ablation experiments, shown in Table 3 and Table 4. We can see that observations from quantum oracles are much closer to the true function value than observations from the classical query, showing great quality of QME.

References

- Wainwright, M. J. 2019. *High-Dimensional Statistics: A Non-Asymptotic Viewpoint*. Vol. 48. Cambridge University Press.
- Gilyén, A.; Su, Y.; Low, G. H.; and Wiebe, N. 2019. Quantum singular value transformation and beyond: exponential improvements for quantum matrix arithmetics. In *Proceedings of the Annual ACM SIGACT Symposium on Theory of Computing*, 193–204.